Subcritical crack growth and long-term strength in rock and cementitious material

Yoshitaka NARA[1, 2*], Masafumi TAKADA[3], Daisuke MORI[4], Hitoshi OWADA[5], Tetsuro YONEDA[1], Katsuhiko KANEKO[1]

[1] Graduate School of Engineering, Hokkaido University, Kita 13 Nishi 8, Kita-ku, Sapporo 060-8628, Japan

[2] Department of Earth Sciences, University College London, Gower Street, London WC1E 6BT, United Kingdom

[3] Graduate Student, Hokkaido University, Kita 13 Nishi 8, Kita-ku, Sapporo 060-8628, Japan (Present address: JGC Corporation, 2-3-1, Minato Mirai, Nishi-ku, Yokohama 220-6001, Japan)

[4] Taiheiyo Consultant Co., Ltd., Ohsaku, Sakura 285-8655, Japan

[5] Radioactive Waste Management Funding and Research Center, Cyuou-ku, Tokyo 104-0052, Japan

*Corresponding author: Yoshitaka Nara

E-mail: nara@geo-er.eng.hokudai.ac.jp

TEL&FAX: +81-11-706-6325

Abstract

High-strength and ultra low-permeability concrete (HSULPC) is a strong candidate for a radioactive waste package containing transuranic radionuclides (TRU waste) for geological disposal. Knowledge of the time-dependent fracturing of HSULPC and surrounding rock mass is essential to assess the long-term stability of such underground repositories. We have measured crack velocity in andesite and HSULPC both in air and water to examine subcritical crack growth by the Double-Torsion method. In air, the crack velocity in andesite increased when the temperature and relative humidity increased. On the other hand, the temperature and relative humidity had little effect on the crack velocity in HSULPC in air. In water, the crack velocity increased when the temperature was higher for both andesite and HSULPC. Using these experimental results, the long-term strength was estimated. It was shown that the long-term strength of HSULPC was higher than that of andesite. In air, the long-term strength for andesite was affected by the temperature and relative humidity. The long-term strength for andesite decreased when the temperature or relative humidity increased. For HSULPC, the change of the long-term strength with varying temperature or relative humidity was smaller than andesite in air. In water, the long-term strength for both materials decreased with increasing the temperature. Comparing the long-term strength of andesite and HSULPC at the same environmental conditions, it was recognized that the decrease of the long-term strength of HSULPC is smaller than that of andesite. The long-term strength in water was smaller than that in air for both materials.

Key words: Subcritical Crack Growth, Long-Term Strength, Double-Torsion Method, Andesite, High-Strength and Ultra Low-Permeability Concrete, Environmental Dependence

1. Introduction

Recent civil engineering projects have used underground rock mass as, for example, repositories for radioactive wastes, underground power plants or caverns for storing liquid natural gas (LNG) or liquid petroleum gas (LPG). Long-term stability is required for these structures. In the construction of structures in rock mass, estimates of the long-term strength or time-to-failure are necessary. Since knowledge of the time-dependent fracturing of rock is essential to evaluate the long-term strength or time-to-failure, the investigation of time-dependent fracturing of rock is necessary. Therefore, the investigation of time-dependent crack growth has been extensively conducted to estimate the long-term strength and time-to-failure (Wilkins 1980; Lajtai and Schmidtke 1986; Miura et al. 2003; Jeong et al. 2003a, 2007).

For geological disposal of radioactive wastes, the intensity of radioactivity of radionuclides can be reduced by engineered barriers such as bentonite buffer and by natural barriers such as a rock mass. If the repository of radioactive wastes is located in an area where the hydraulic gradient and the permeability are high, the retardation of migration of radionuclides by these barriers may not be enough. Therefore, the influences of nuclides with low adsorption, such as I-129 and C-14, will be large. In order to retard the migration, several alternative concepts of radioactive waste packages are being developed (Owada et al. 2005). It is planned that high-strength and ultra low-permeability concrete (HSULPC) will be used for a radioactive waste package for the geological disposal of transuranic radionuclides (TRU waste) (Kawasaki et al. 2005; Owada et al. 2005; Shibuya et al. 2005). Fig. 1 shows a schematic illustration of this alternative concept using HSULPC. The aim of this scheme is to confine radionuclide, especially C-14, for a long term. It is supposed that C-14 is confined for 60000 years, which corresponds to 10 times of the half-life of C-14. If a crack nucleates and propagates in HSULPC, however, the confining ability of the package can decline after crack growth for the long term even though the crack velocity is low. Therefore, research on time-dependent fracturing of HSULPC is important for radioactive waste disposal.

Classical fracture mechanics postulates that a crack propagates rapidly once the critical stress intensity factor (fracture toughness) has been reached. The crack can

advance slowly even when the stress intensity factor is lower than the critical stress intensity factor. This phenomenon is called “subcritical crack growth” (Atkinson 1984; Atkinson and Meredith 1987a; Salganik et al. 1997), which is one of the main causes of time-dependent behaviour. In rock, a thermally activated chemical reaction between the siloxane bond and water has been considered one of the main mechanisms of subcritical crack growth (Atkinson and Meredith 1987a). Therefore, it is worth investigating the effect of the temperature, humidity or water on subcritical crack growth. In HSULPC, the mechanism of subcritical crack growth is unknown. Ishijima et al. (2008) noted the possibility of temperature and humidity changes in the underground. Additionally, water may reach the package. Therefore, it is important to investigate the effects of temperature, relative humidity and water on subcritical crack growth in HSULPC.

The Double-Torsion (DT) method (Evans 1972) is one of the typical methods of fracture mechanics to measure subcritical crack growth. For the DT method, the stress intensity factor is independent of the crack length. Therefore, the DT method is convenient for opaque materials such as rock and has been used by many researchers (Atkinson and Meredith 1987b; Nara 2007). The DT method is also considered to be convenient for cementitious material and has been used in several studies: for example, on cement paste (Mindess and Nadeau 1974; Nadeau et al. 1974; Beaudoin 1985), portland cement mortar (Wecharatana and Shah 1980), calcium silicate hydrate (Beaudoin et al. 1998), and the mixture of calcium silicate hydrate and calcium hydroxide (Beaudoin et al. 1998). For HSULPC, however, subcritical crack growth has never been studied and the DT method has not used either.

In the case of both rock and HSULPC, it is important to decide the experimental procedure and the loading condition for the DT method (Nara and Kaneko, 2005, 2006). Then, we measure subcritical crack growth in HSULPC and consider the crack growth mechanism.

In this study, subcritical crack growth in rock and HSULPC was investigated. Mainly, the relations between crack velocity and stress intensity factor were investigated experimentally. Specifically, the effects of temperature, relative humidity and water were investigated. By using the results of subcritical crack growth measurements, the long-term strength of rock and HSULPC was estimated.

2. Samples

2.1. Rock sample

Kumamoto andesite was used as a rock sample in this study. The quarry of Kumamoto andesite is in Kumamoto prefecture, Southwest Japan. Kumamoto andesite is porphyritic, and consists of plagioclase (50 ~ 60 %), hornblende (2 ~ 3 %), augite (2 ~ 3 %) as phenocrysts and fine-grained groundmass. Some phenocrysts of 1~2 mm in length were distributed in the groundmass. There was no preferred orientation of the crystal axis for the phenocryst and pore shape (Jeong et al. 2003b, 2007).

The porosity of this rock measured by water saturation was 7 %.

P-wave velocities in three orthogonal directions were 4.8 km/s (Nara and Kaneko 2005). Therefore, this rock is considered isotropic.

The uniaxial compressive strength was 151 MPa. The Young's modulus and Poisson's ratio determined from the tangential line of the stress-strain curve at the point of 50 % of the uniaxial compressive strength were 31.9 GPa and 0.27, respectively. Therefore, the shear modulus was determined 12.6 GPa. The Brazilian tensile strength measured by Jeong et al. (2003a) was 9.5 MPa.

2.2. Cementitious sample

As mentioned before, HSULPC was used as a sample of cementitious material. In Table 1, the composition of HSULPC is shown. After placing concrete in a mold and being kept for 2 days in air at a temperature of 293 K, HSULPC cured under the condition of steam curing at a temperature of 363 K for 2 days. This curing procedure is different from the curing for usual cementitious material which reaches its final strength after curing for 28 days. This curing is used in order that HSULPC reached its final strength much earlier than usual cementitious material. The final strength was achieved just after the steam curing and kept constant. All of specimens of HSULPC were used in several months after curing.

The porosity of HSULPC measured by mercury porosimetry was 5 % (Kawasaki et al. 2005). The water permeability coefficient was 4×10^{-19} m/s (Kawasaki et al. 2005).

P-wave velocities in three orthogonal directions were 5.0 km/s. Therefore, this material is also considered isotropic.

The uniaxial compressive strength was 203 MPa. The Young's modulus and Poisson's ratio determined from the stress-strain curve under uniaxial compression were 50.9 GPa and 0.20, respectively. Therefore, the shear modulus was determined 21.2 GPa. The Brazilian tensile strength was 10.9 MPa.

3. Methodology

3.1. Experimental method

The DT method was adopted in this study. The geometry of the specimen and the loading configuration of the DT method are shown in Fig. 2. As shown in this figure, the specimen is a rectangular plate that often includes a guide groove to control the path of the crack propagation in the central part of the specimen (Raju 1981). According to Pletka et al. (1979), the scattering of experimental results were smaller when the specimen had the guide groove only on upper or lower side. Considering the report of Pletka et al., we put the groove on the upper side. In Fig. 2, four thick arrows show the loading forces which are applied at the end of the specimen.

The DT method includes three different testing methods, each of which possesses a different loading procedure. Kies and Clark (1969) introduced the constant load (CL) method for the original DT method. Two other methods, constant displacement rate (CDR) method and load relaxation (RLX) method were introduced by Evans (1972). In the RLX method, the displacement of the loading point is kept constant during the experiment and the load relaxation due to crack propagation is measured. Because the stress intensity factor is a function of the load and the crack velocity is a function of the temporal load and decreasing rate of the load, the relation between the stress intensity factor and the crack velocity can be obtained over a wide range of loads using a single experimental run. For this reason, the RLX method was adopted to measure subcritical crack growth in this study.

For isotropic materials, the stress intensity factor, K_{I}, and crack velocity, da/dt, are expressed as follows (Evans 1973; Williams and Evans 1973):

$$K_{\mathrm{I}} = P w_{\mathrm{m}} \sqrt{\frac{3(1+\nu)}{W d^3 d_{\mathrm{n}}}} \qquad (1)$$

$$\frac{\mathrm{d}a}{\mathrm{d}t} = -\phi_{\mathrm{c}} \times \frac{W d^3 G}{3 w_{\mathrm{m}}{}^2} \frac{S_{\mathrm{i}} P_{\mathrm{i}}}{P^2} \frac{\mathrm{d}P}{\mathrm{d}t} \qquad (2)$$

where P is the applied load, w_{m} is the moment arm (18 mm in this study), ν is Poisson's ratio, W is the width of the specimen, d is the thickness of the specimen, d_{n} is the reduced thickness of the specimen, P_{i} is the initial value of the applied

load, S_i is the compliance of the specimen at the initial crack length a_i, dP/dt is the load relaxation rate, and G is the shear modulus (Williams and Evans 1973). φ_c is a constant that is dependent on the shape of the crack front. Experiments using glass (Williams and Evans 1973) and quartz (Atkinson 1979a) suggested that φ_c = 0.2.

It is important to consider the applicability of Eqs. (1) and (2), because these are approximate solutions based on a thin-plate assumption (Williams and Evans 1973). The size of the DT specimen has to satisfy the condition as follows (Evans et al. 1974; Atkinson 1979b; Pletka et al. 1979):

$$12d \le W \le L/2 \qquad (3)$$

where L is the length of the specimen.

According to the finite element analysis by Trantina (1977), the stress intensity factor is independent of the crack length over the next range:

$$0.55W < a < L - 0.65W . \qquad (4)$$

Ciccotti and his co-workers have reported an analytical approach to DT RLX method using finite element analysis (Ciccotti 2000; Ciccotti et al. 2000a, 2000b, 2001). They expressed the corrective factor of the specimen compliance to consider the non-linear terms of the dependence of the compliance on the crack length in a DT specimen (Ciccotti 2000; Ciccotti et al. 2000a). Additionally, based on their results, they used thicker specimens (W : d = 8 : 1) than those recommended by Evans et al. (1974) or Atkinson (1979b) (Ciccotti et al. 2000b, 2001). Recently, Madjoubi et al. (2007) reported that the applicability of Eqs. (1) and (2) was conditioned by using longer specimen by experiments with soda-lime glass. Sano (1988) reported that the stress intensity factor is independent of the crack length by showing the proportional relation between the compliance and the crack length in DT specimen of soda-lime glass, basalt and quartz andesite.

Taking these restrictions into account, the size of the specimens in this study shown in Fig. 2 was set to the width W = 45 [mm], the thickness d = 3 [mm], the reduced thickness d_n = 2 [mm], and the length L =150 [mm].

The DT specimen used in this study had a single rectangular guide groove on the upper plane (see Fig. 2). Nara (2004) reported that crack propagation was not controlled if the width of the groove was less than the mean grain size of the material. Because some phenocrysts had the length of 2 mm in Kumamoto andesite, the width of the guide groove was set as 2 mm for andesite. On the other

hand, the width of the groove for HSULPC was 1 mm, as the grain size was less than 1 mm.

3.2. Experimental apparatus

Measurements were conducted in air and water in this study. Schematic illustration of the apparatus used for the measurements in water is shown in Fig. 3. The apparatus in air is the same one used by Nara and Kaneko (2005, 2006) and Nara et al. (2006, 2009).

The DT specimen is loaded by the electrical-powered cylinder via stainless steel balls. The diameter of the balls is 4 mm. For the experiment in air, crack propagation in the DT specimen can be monitored by the digital microscope placed under the specimen. The applied load is measured by the load cell with the accuracy of 0.04 N. Displacement of the loading point is measured by two displacement transducers with the accuracy of 0.5 μm.

The apparatus is set up in a temperature and humidity controlled room. The temperature and relative humidity can be kept constant within 0.1 K in the range of 283 to 353 K and within 1 % in the range of 40 to 90 %, respectively.

3.3. Experimental condition

Measurements of subcritical crack growth in air were conducted with different temperature at the same relative humidity or with different relative humidity at the same temperature to investigate the effect of the temperature or relative humidity. Most of measurements were conducted under controlled temperature and relative humidity. However, some measurements were carried out under low relative humidity (25 ~ 26 % of relative humidity with the temperature of 291 ~ 292 K) which we cannot control. This was the surrounding environmental condition of the laboratory in winter. The measurements under this condition were carried out without controlling the temperature and relative humidity.

Measurements in water were conducted at various temperatures. The temperature of the water was controlled by controlling the temperature in air.

Measurements for rock were carried out in distilled water. Generally water becomes alkaline when cementitious materials are immersed. The measurements for HSULPC in water were therefore conducted with water which showed alkalinity as several pieces of HSULPC had been kept in that water (originally distilled water) for more than 2 months.

3.4. Experimental procedure

At first, precracking was conducted with the apparatus in air. For precracking, load was applied to the specimen slowly, occasionally fixing the displacement of the loading points. During this operation, crack propagation was monitored with the digital microscope set under the specimen, and we decreased the load rapidly when the crack length reached 25mm, which is the minimum length required for the condition in which the stress intensity factor is independent of the crack length for a DT specimen in this study, according to Trantina (1977).

After precracking, the temperature and relative humidity in the testing room were set and kept constant. The apparatus and the DT specimen were exposed to the testing environment for 20 hours. After this, crack growth was measured by the DT RLX method.

In this measurement, we slowly applied a preload of 14 ~ 16 N, which corresponded to 15 ~ 25 % of the maximum load (initial load P_i in Eq. (2)). Then we applied a large displacement rapidly to the loading points of the specimen and held it constant throughout the measurement. This large displacement has to be decided so that the maximum load in DT RLX method (P_i in Eq. (2)) approaches the value corresponding to the fracture toughness (Nara and Kaneko 2005, 2006). This displacement was 0.27 mm for Kumamoto andesite in all conditions as specified by Nara and Kaneko (2005).

For HSULPC, the fracture toughness was measured by the DT CDR method with a displacement rate of 0.23 mm/s, which is the maximum rate of the apparatus. The measured fracture toughness was 1.62 $MN/m^{3/2}$. Based on this result, the displacement of the loading point for HSULPC in air was set as 0.27 mm. With this displacement, the maximum load reached more than 90 % of the load which corresponds to the fracture toughness.

For HSULPC in water, however, the specimen was broken and the measurement was impossible with the displacement of 0.27 mm. In this case, the displacement must be reduced. Therefore, the displacement was set as 0.24 mm in water at 285 K and 328 K. In the experiment in water at 348K, the specimen was broken with the displacement of 0.24 mm. We therefore reduced the displacement more in this case and it was set as 0.21 mm in for the experiment in water at 348K.

In Fig. 4, the temporal change of the load is shown. Although the change within 200 seconds is shown in this figure, all experiments were conducted for 1.5 ~ 2 hours.

4. Results

In this study, the relation between the stress intensity factor K_I and the crack velocity da/dt (K_I-da/dt relation) is evaluated by using the equation (Charles 1958):

$$\frac{da}{dt} = AK_I^n \qquad (5)$$

where A and n are constants determined experimentally. n is known as the subcritical crack growth index.

4.1 Results for rock

Figs. 5 and 6 show K_I-da/dt relations for andesite obtained in air, which show the effects of temperature and relative humidity, respectively. From these figures, it is shown that the crack velocity increases when the temperature or relative humidity increases. It is considered that the crack velocity in andesite in air is affected by both the temperature and relative humidity.

In Fig. 7, K_I-da/dt relations for andesite obtained in distilled water are shown. From this figure, it is shown that the crack velocity increases when the temperature increases. It is considered that the crack velocity in andesite in water is affected by the temperature of water.

The results of subcritical crack growth measurements are summarized in Tables 2 ~ 4. The stress intensity factor at da/dt = 10^{-6} [m/s], $K_I(10^{-6})$, is listed in these tables to provide a quantitative comparison of the stress intensity factor, because the range of the crack velocity was 10^{-2} ~ 10^{-8} m/s. Since the range of the stress intensity factor for Kumamoto andesite shown in Fig. 5 was approximately 1.2 ~ 1.7 MN/m$^{3/2}$, the crack velocity at K_I = 1.4 [MN/m$^{3/2}$], da/dt(1.4), is listed in Table 2 to provide a quantitative comparison of the crack velocity. In the same way, da/dt(1.5) is listed in Table 3 to provide a quantitative comparison, because the range of the stress intensity factor for Kumamoto andesite shown in Fig. 6 was approximately 1.2 ~ 1.9 MN/m$^{3/2}$. For the result in water, da/dt(1.1) is listed in Table 4 to provide a quantitative comparison, because the range of the stress intensity factor shown in Fig. 7 was approximately 0.9 ~ 1.4 MN/m$^{3/2}$. From Tables 2 ~ 4, it is shown that the stress intensity factor decreases and the crack

velocity increases when the temperature or relative humidity increases. These results agree with the concept that subcritical crack growth in rock is activated thermally and water has a significant effect (Anderson and Grew 1977; Atkinson 1984; Atkinson and Meredith 1987a).

From Tables 2 ~ 4, it is shown that the value of subcritical crack growth index n tends to be smaller when the temperature or relative humidity is higher. It may be probable that n is dependent on the environmental condition.

4.2 Results for cementitious material

Figs. 8 and 9 show K_I-da/dt relations for HSULPC obtained in air. It is shown that the dependence of the crack velocity on the temperature or relative humidity is not clear. It is considered that the temperature and relative humidity have little effect on the crack velocity in HSULPC.

In Fig. 10, K_I-da/dt relations for HSULPC in water with different temperatures are shown. This figure shows that the crack velocity increases with increasing temperature. It is considered that the temperature has a significant effect on the crack velocity in HSULPC in water.

In Tables 5 ~ 7, the results of subcritical crack growth measurements are summarized. As mentioned in *4.1.*, the stress intensity factor at da/dt = 10^{-6} [m/s], $K_I(10^{-6})$, is listed in these tables to provide a quantitative comparison of the stress intensity factor. The crack velocity at K_I = 1.3 [MN/m$^{3/2}$], da/dt(1.3), is listed in Table 5 to provide a quantitative comparison of the crack velocity, because the range of the stress intensity factor for HSULPC shown in Fig. 8 was approximately 1.2 ~ 1.5 MN/m$^{3/2}$. Similarly, da/dt(1.35) is listed in Table 6 to provide a quantitative comparison, because the range of the stress intensity factor for Kumamoto andesite shown in Fig. 9 was approximately 1.3 ~ 1.45 MN/m$^{3/2}$. For the result in water, da/dt(1.1) is listed in Table 7 to provide a quantitative comparison, because the range of the stress intensity factor shown in Fig. 10 was approximately 0.9 ~ 1.4 MN/m$^{3/2}$. From Tables 5 and 6, the changes of the stress intensity factor and crack velocity are not significant even though the temperature or relative humidity in air changes considering the standard deviation. On the other hand, it is clear that the value of the stress intensity factor decreases and the

crack velocity increases obviously when the temperature in water increases from Table 7. It is considered that the temperature has a strong effect on subcritical crack growth in HSULPC in water.

It is shown from Tables 5 ~ 7 that the value of subcritical crack growth index n tends to be smaller when the temperature or humidity increases. It may be that n for HSULPC is dependent on environmental conditions. Additionally, it is clear that n for HSULPC is higher than that for andesite.

4.3 Long-term strength

It is possible to estimate the long-term strength of material by using the results of subcritical crack growth measurements. Estimation of the long-term strength predicts the strength or the time-to-failure of a material with applied load in future.

We consider the situation of an infinite plate containing a single crack, subjected to an uniform tensile stress. The long-term strength can be estimated by the following equation (see Appendix):

$$S_t(x) = \left\{ \frac{1}{3.15\times10^7 x} \frac{2}{(n-2)\pi A} \right\}^{1/n} \left(\frac{K_{IC}}{S_t} \right)^{(2-n)/n} \qquad (6)$$

where K_{IC} is the fracture toughness, S_t is the strength, x is the time-to-failure [years], and $S_t(x)$ is the long-term strength. For the value of the strength, we used the values of Brazilian tensile strength mentioned in Section 2 to calculate the long-term strength using Eq. (6).

The relations between the time-to-failure and the long-term strength for andesite and HSULPC are shown in Fig. 11. Figs. 11(a) and (b) show the relations in air with different temperature and different relative humidity, respectively. Fig. 11(c) shows the relations in water. From these figures, it is shown that the long-term strength of HSULPC is larger than that of andesite in all cases. From Figs. 11(a) and (b), it is clear that the change of the long-term strength for HSULPC with varying temperature or relative humidity is smaller than andesite in air. From Fig. 11(c), it is shown that the long-term strength for both materials decreases with increasing the temperature in water. Comparing the results at a same

environmental condition, it is recognized that the decrease of the long-term strength of HSULPC is smaller than that of andesite.

Additionally, it is recognized that the long-term strength in water was smaller than that in air for both materials.

5. Discussion

It is considered that the crack velocity in rock is affected by the environmental conditions. Meredith and Atkinson (1985) reported that the crack velocity increased with increasing water vapour pressure. Waza et al. (1980) and Sano and Kudo (1992) reported that the crack velocity increased in water by using andesite and granite. This study supports these results. Also, stress corrosion (Anderson and Grew 1977) seems to affect subcritical crack growth in rock.

On the other hand, the main mechanism of subcritical crack growth in HSULPC seems to be different from rock. In air, the crack velocity was not affected by the change of the temperature and relative humidity. According to Uzawa et al. (1998), even when the concrete was cured by steam curing at 353K and then cured again under higher temperature, the strength of concrete did not change significantly. Hence, it is considered that the strength of the concrete does not change under lower temperature. The experimental conditions in air can have little effect on the crack velocity in HSULPC due to the higher curing temperature than temperature in experiments.

Comparing K_I-da/dt relations in Fig. 10 to those in Fig. 8 or Fig. 9, it is recognized that the crack velocities in water are higher than those in air. Ranjith et al. (2008) reported that when the concrete was fully wet, the strength reduced significantly in comparison with the strength of dry concrete. Results in this study are consistent with the result by Ranjith et al. It is important to consider the reason why water has a remarkable effect on the crack growth in cementitious material.

The loss of strength due to the leaching of calcium was reported by Carde and François (1997) and Heukamp et al. (2001). Since the crack velocity in HSULPC increased with increasing temperature only in water, it is considered that subcritical crack growth in HSULPC happens due to leaching of calcium at the crack tip. Additionally, the rate of leaching for calcium is dependent on the temperature of water (Kamali et al. 2008). Due to these effects, the dependence of the crack velocity in HSULPC on the temperature of water was considered to be observed.

The estimation of the long-term strength reflects subcritical crack growth measurements. From Fig. 11, it is clear that the decrease of the long-term strength for HSULPC is lower than that of andesite. The slope of the relation between the

long-term strength and time-to-failure is expressed by 1/*n* (see Eq. (6)). The small decrease of the long-term strength for HSULPC is therefore due to the high value of *n* of HSULPC.

From Fig. 11, it is recognized that the decrease of the long-term strength for HSULPC in water is larger than in air and depends on the temperature. This result reflects the dependence of subcritical crack growth in HSULPC in water on the temperature. Similar tendency is observed for andesite. Therefore, it is considered that water remarkably affects the long-term strength and control or shut-off of water is important to lengthen the life-time of rock and cementitious material.

It is essential to calculate the long-term strength of HSULPC in 60000 years in various conditions. For this purpose, consideration of the dependence of constants *n* and *A* on the temperature and humidity is necessary. The relations between environmental conditions and *n* or log*A* are shown in Figs. 12 ~ 14. Figs. 12, 13 and 14 show the relations obtained in air with different temperature at constant relative humidity, in air with different relative humidity at constant temperature, and in water, respectively. As shown in these figures, the following relations were obtained with the least square approximation:

$$\left.\begin{aligned} n &= -0.83T + 380 \\ \log A &= 0.080T - 45.8 \end{aligned}\right\} \quad \text{(in air at constant relative humidity)} \qquad (7)$$

$$\left.\begin{aligned} n &= -1.21h_r + 260 \\ \log A &= 0.171h_r - 41.2 \end{aligned}\right\} \quad \text{(in air at constant temperature)} \qquad (8)$$

$$\left.\begin{aligned} n &= -1.36T + 526 \\ \log A &= 0.220T - 81.2 \end{aligned}\right\} \quad \text{(in water)} \qquad (9)$$

where h_r is the relative humidity [%]. By using these equations, we can evaluate *n* and log*A* under various environmental conditions. Additionally, by substituting these values to Eq. (6), we can calculate the long-term strength under various environmental conditions.

In Fig. 15, the relations between the long-term strength in 60000 years calculated with using Eqs. (6) ~ (9) and environmental conditions are shown. Figs. 15(a), (b), and (c) show the relations in air at constant relative humidity, in air at constant temperature, and in water, respectively. In these figures, the estimations obtained from each experiment are also shown with solid symbols. The maximum differences between the long-term strength calculated with Eqs. (6) ~ (9) and that from experimental results were 0.65 MPa, 0.47 MPa, and 0.43 MPa in Figs. 15(a),

(b), and (c), respectively. These differences are shown as error bars in Fig. 15. From these figures, it is clear that the effect of environment on the long-term strength of HSULPC is remarkable in water. The long-term strength in 60000 years decreases significantly with increasing the temperature in water. It is considered that the control of water content is necessary for larger long-term strength or longer time-to-failure. If possible, it is desirable to keep HSULPC dry for long-term stability.

The long-term strength estimated in this study is based on the situation that the stress intensity factor increases with increasing crack length. On the other hand, it is possible that the stress intensity factor decreases with increasing crack length (Kachanov 1982; Touzet et al. 2006). Therefore, the long-term strength estimated in this study may be too small. However, to ensure the long-term stability of structures which will be used for a long time, this estimation is considered to be necessary. To estimate the long-term strength more precisely, it is necessary to consider the effects of the temporal change of the temperature, relative humidity, or water content. These will be the subject of future work.

6. Conclusion

In this study, subcritical crack growth in andesite and HSULPC was investigated experimentally by using the DT method. The effects of environmental conditions (temperature, relative humidity and water) were investigated from the experiments in air and water.

For andesite, it was shown that both the temperature and relative humidity in air affected the crack velocity remarkably. When the temperature or relative humidity increased, the crack velocity at the same stress intensity factor increased. On the other hand, both the temperature and relative humidity in air had little effect on the crack velocity in HSULPC. In water, the crack velocity both in andesite and HSULPC increased with increasing the temperature.

By using the results of subcritical crack growth measurement, the long-term strength of andesite and HSULPC was evaluated. It was shown that the long-term strength of HSULPC was higher than that of andesite. In air, the long-term strength for andesite was affected by the temperature and relative humidity. When the temperature or relative humidity increased, the long-term strength for andesite decreased. The change of the long-term strength for HSULPC with changing the temperature or relative humidity in air was smaller than for andesite. In water, it was shown that the long-term strength for both materials decreased with increasing the temperature. Comparing the long-term strength of andesite and HSULPC at a same environmental condition, it was recognized that the decrease of the long-term strength of HSULPC is smaller than that of andesite. The long-term strength in water was smaller than that in air for both materials.

It was clarified that water had a strong effects on subcritical crack growth and the long-term strength of both rock and cementitious material. It is concluded that the control of water content is necessary for larger long-term strength of these materials.

Appendix. Estimation of the long-term strength

In this study, we considered a situation where an infinite plate containing a single crack is subjected to an uniform tensile stress σ_{yy}^{∞}. In this case, the stress intensity factor is expressed as follows:

$$K_{\mathrm{I}} = \sigma_{yy}^{\infty}(\pi a)^{1/2}. \qquad \text{(A.1)}$$

If the K_{I}-da/dt relation is expressed with Eq. (5), the following equation can be obtained:

$$\frac{\mathrm{d}a}{\mathrm{d}t} = \pi^{n/2} A \sigma_{yy}^{\infty n} a^{n/2}. \qquad \text{(A.2)}$$

From Eq. (A.2), the following equation can be obtained:

$$\int a^{-n/2}\mathrm{d}a = \int \pi^{n/2} A \sigma_{yy}^{\infty n}\mathrm{d}t. \qquad \text{(A.3)}$$

The general solution of Eq. (A.3) is as follows:

$$\frac{1}{1\text{-}n/2} a^{1-n/2} = \pi^{n/2} A \sigma_{yy}^{\infty n} t + c \qquad \text{(A.4)}$$

where c is a constant of integration. Assuming that $a = a_0$ when $t = 0$, the constant c can be determined from Eq. (A.4) as follows:

$$\frac{2}{2\text{-}n} a_0^{(2-n)/2} = c. \qquad \text{(A.5)}$$

Substituting Eq. (A.5) into Eq. (A.4), the following equation can be obtained:

$$a^{(2-n)/2} = \frac{2-n}{2}\pi^{n/2} A \sigma_{yy}^{\infty n} t + a_0^{(2-n)/2}. \qquad \text{(A.6)}$$

From Equation (A.6), the following equation can be obtained:

$$t = \frac{2}{(n-2)\pi^{n/2} A}\frac{a_0^{(2-n)/2}}{\sigma_{yy}^{\infty n}}\left\{1-\left(\frac{a}{a_0}\right)^{(2-n)/2}\right\}. \qquad \text{(A.7)}$$

Even though the crack propagates statically, the manner of the crack propagation will change from static to dynamic as time goes by and the crack length will diverge. Assuming that the time when the crack length diverges is called as "time-to-failure", t_{f}, this can be expressed as follows:

$$t_{\mathrm{f}} = \frac{2}{(n-2)\pi^{n/2} A}\frac{a_0^{(2-n)/2}}{\sigma_{yy}^{\infty n}}. \qquad \text{(A.8)}$$

Considering the situation that a material reaches failure in x years under a constant stress, this stress can be defined as "long-term strength", $S_{\mathrm{t}}(x)$. Since the time-to-

failure is x years ($3.15\times10^7 x$ seconds) under this stress, the following equation can be obtained from Equation (A.8):

$$(S_t(x))^n = \frac{1}{3.15\times10^7 x}\frac{2}{(n-2)\pi^{n/2}A}a_0^{(2-n)/2}. \qquad \text{(A.9)}$$

Assuming that the tensile strength and the fracture toughness of a material are S_t and K_{IC}, respectively, when the crack length is a_0, the relation between S_t and K_{IC} can be expressed as follows:

$$K_{IC} = S_t(\pi a_0)^{1/2}. \qquad \text{(A.10)}$$

From Eqs. (A.9) and (A.10), the following equation can be obtained:

$$S_t(x) = \left\{\frac{1}{3.15\times10^7 x}\frac{2}{(n-2)\pi A}\right\}^{1/n}\left(\frac{K_{IC}}{S_t}\right)^{(2-n)/n}. \qquad \text{(A.11)}$$

The long-term strength can be estimated by using this equation.

Acknowledgement

This study includes a part of the result of “Research and development of processing and disposal technique for TRU waste containing I-129 and C-14” under a grant from the Ministry of Economy, Trade and Industry. The authors appreciate the support of Research Fellowships of the Japan Society for the Promotion of Science for Young Scientists. Additionally, we appreciate Dr. Ben Lishman at University College London for reading this manuscript and for useful comments.

References

Anderson OL, Grew PC (1977) Stress corrosion theory of crack propagation with applications to geophysics. Rev Geophys Space Phys 15:77-104

Atkinson BK (1979a) A fracture mechanics study of subcritical tensile cracking of quartz in wet environments. Pure Appl Geophys 117:1011-1024

Atkinson BK (1979b) Fracture toughness of Tennessee sandstone and Carrara marble using the double torsion testing method. Int J Rock Mech Min Sci & Geomech Abstr 16:49-53

Atkinson BK (1984) Subcritical crack growth in geological materials. J Geophys Res 89:4077-4114

Atkinson BK, Meredith PG (1987a) The theory of subcritical crack growth with applications to minerals and rocks. In: Atkinson BK (ed) Fracture mechanics of rock, Academic Press, London, pp 111-166

Atkinson BK, Meredith PG (1987b) Experimental fracture mechanics data for rocks and minerals. In: Atkinson BK (ed) Fracture mechanics of rock, Academic Press, London, pp 477-525

Beaudoin JJ (1985) Effect of humidity on subcritical crack growth in cement paste. Cem Concr Res 15:871-878

Beaudoin JJ, Gu P, Myers RE (1998) The fracture of C-S-H and C-S-H/CH mixture. Cem Concr Res 28:341-347

Carde C, François R (1997) Effect of the leaching of calcium hydroxide from cement paste on mechanical and physical properties. Cem Concr Res 27:539-550

Charles RJ (1958) Static fatigue of glass. II. J Appl Phys 29:1554-1560

Ciccotti M (2000) Realistic finite-element method for the double-torsion loading configuration. J Am Ceram Soc 83:2737-2744

Ciccotti M, Gonzato G, Mulargia F (2000a) The double torsion loading configuration for fracture propagation: an improved methodology for the load-relaxation at constant displacement. Int J Rock Mech Min Sci 37:1103-1113

Ciccotti M, Negri N, Sassi L, Gonzato G, Mulargia F (2000b) Elastic and fracture parameters of Etna, Stromboli, and Vulcano lava rocks. J Volcanol Geother Res 98:209-217

Ciccotti M, Negri N, Gonzato G, Mulargia F (2001) Practical application of an improved methodology for the double torsion load relaxation method. Int J Rock Mech Min Sci 38:569-576

Evans AG (1972) A method for evaluating the time-dependent failure characteristics of brittle materials – and its application to polycrystalline alumina. J Mater Sci 7:1137-1146

Evans AG (1973) A simple method for evaluating slow crack growth in brittle materials. Int J Fract 9:267-275

Evans AG, Linzer M, Russell LR (1974) Acoustic emission and crack propagation in polycrystalline alumina. Mater Sci Eng 15:253-261

Heukamp FH, Ulm FJ, Germaine JT (2001) Mechanical properties of calcium-leached cement pastes: Triaxial stress states and the influence of the pore pressure. Cem Concr Res 31:767-774

Ishijima Y, Fujii Y, Ichihara Y, Kodama J (2008) Closure of oldworking in Kushiro coal mine and its mechanism. Journal of MMIJ 124:435-444 (in Japanese with English abstract)

Jeong HS, Obara Y, Sugawara K (2003a) The strength of rock under water vapour pressure. Journal of MMIJ 119:9-16 (in Japanese with English abstract)

Jeong HS, Nara Y, Obara Y, Kaneko K (2003b) Stress corrosion index of Kumamoto andesite estimated from two types of experimental method. In: Proceedings of International Symposium on the Fusion Technology of Geosystem Engineering, Rock Engineering and Geophysical Exploration, pp 221-228

Jeong HS, Kang SS, Obara Y (2007) Influence of surrounding environments and strain rates on the strength of rocks subjected to uniaxial compression. Int J Rock Mech Min Sci 44:321-331

Kachanov ML (1982) Microcrack model of rock inelasticity Part III: Time-dependent growth of microcracks. Mech Mater 1:123-129

Kamali S, Moranville M, Leclercq S (2008) Material and environmental parameter effects on the leaching of cement pastes: Experiments and modelling. Cem Concr Res 38:575-585

Kawasaki T, Asano H, Owada H, Otsuki A, Yoshida T, Matsuo T, Shibuya K, Takei A (2005) Development of waste package for TRU-disposal(4) - Evaluation of confinement performance of TRU waste package made of High-

Strength and Ultra Low-Permeability concrete-. In: Proceedings of GLOBAL 2005, No 254

Kies JA, Clark ABJ (1969) Fracture propagation rates and times to fail following proof stress in bulk glass. In: Plat PL (ed) Fracture 1969, Chapman and Hall, London, pp 483-491

Lajtai EZ, Schmidtke RH (1986) Delayed failure in rock loaded in uniaxial compression. Rock Mech Rock Eng 19:11-25

Madjoubi MA, Hamidouche M, Bouaouadja N (2007) Experimental evaluation of the double torsion analysis on soda-lime glass. J Mater Sci 42:7872-7881

Meredith PG, Atkinson BK (1985) Fracture toughness and subcritical crack growth during high-temperature tensile deformation of Westerly granite and Black gabbro. Phys Earth Planet Inter 39:33-51

Mindess S, Nadeau JS (1974) Effects of different curing conditions on slow crack growth in cement paste. Cem Concr Res 4:953-965

Miura K, Okui Y, Horii H (2003) Micromechanics-based prediction of creep failure of hard rock for long-term safety of high-level radioactive waste disposal system. Mech Mater 35:587-601

Nadeau JS, Mindess S, Hay JM (1974) Slow crack growth in cement paste. J Am Ceram Soc 57:51-54

Nara Y (2004) Study of subcritical crack growth in rock. PhD Thesis, Hokkaido University (in Japanese)

Nara Y (2007) Previous results and new development for studies of subcritical crack growth in rock – To understand time-dependent behavior of crack growth -. Journal of MMIJ 123:2-9 (in Japanese with English abstract)

Nara Y, Kaneko K (2005) Study of subcritical crack growth in andesite using the Double Torsion test. Int J Rock Mech Min Sci 42:521-530

Nara Y, Kaneko K (2006) Sub-critical crack growth in anisotropic rock. Int J Rock Mech Min Sci 43:437-453

Nara Y, Koike K, Yoneda T, Kaneko K (2006) Relation between subcritical crack growth behavior and crack paths in granite. Int J Rock Mech Min Sci 43:1256-1261.

Nara Y, Takada M, Igarashi T, Hiroyoshi N, Kaneko K (2009) Subcritical crack growth in rocks in an aqueous environment. Exploration Geophysics 40:163-171.

Owada H, Otsuki A, Asano H (2005) Development of waste package for TRU-disposal(1) –Concepts and performances-. In: Proceedings of GLOBAL 2005, No 351

Pletka BJ, Fuller Jr ER, Koepke BG (1979) An evaluation of double-torsion testing – Experimental. ASTM STP 678, pp 19-37

Raju KR (1981) Effect of depth of side grooves in double torsion specimens on plane strain fracture toughness. Int J Fract 17:R189-R190

Ranjith PG, Jasinge D, Song JY, Choi SK (2008) A study of the effect of displacement rate and moisture content on the mechanical properties of concrete: Use of acoustic emission. Mech Mater 40:453-469

Salganik RL, Rapoport L, Gotrib VA (1997) Effect of structure on environmentally assisted subcritical crack growth in brittle materials. Int J Fract 87:21-46

Sano O (1988) A revision of the double-torsion technique for brittle materials. J Mater Sci 23:2505-2511

Sano O, Kudo Y (1992) Relation of fracture resistance to fabric for granitic rocks. Pure Appl Geophys 138:657-677

Shibuya K, Asano H, Owada H, Otsuki A, Kawasaki T, Yoshida T, Matsuo T, Takei A (2005) Development of waste package for TRU-disposal(3) - Examination of manufacturing technique of TRU waste package made of High-Strength and Ultra Low-Permeability concrete-. In: Proceedings of GLOBAL 2005, No 256

Touzet M, Le Poulain F, Aubert I, Puiggali M (2006) The incremental self-consistent scheme applied to active stress corrosion cracks. Mech Mater 38:620-632

Trantina GG (1977) Stress analysis of the double-torsion specimen. J Am Ceram Soc 60:338-341

Uzawa M, Hanehara S, Uchikawa H (1998) Microstructure and strength of high-strength mortar cured at various conditions. Cement Science and Concrete Technology 52:96-103 (in Japanese with English abstract)

Waza T, Kurita K, Mizutani H (1980) The effect of water on the subcritical crack growth in silicate rocks. Tectonophys 67:25-34

Wecharatana M, Shah SP (1980) Double Torsion tests for studying slow crack growth of Portland cement mortar. Cem Concr Res 10:833-844

Wilkins BJS (1980) Slow crack growth and delayed failure of granite. Int J Rock Mech Min Sci & Geomech Abstr 17:365-369

Williams DP, Evans AG (1973) A simple method for studying slow crack growth. J Test Eval 1:264-270

Titles of Tables

Figure captions

Fig. 1 The schematic illustration of an alternative concept of the radioactive waste package.

Fig. 2 Double-Torsion specimen and loading configuration. The loading forces are shown by four thick arrows.

Fig. 3 The schematic illustration of experimental apparatus in water.

Fig. 4 The temporal changes of the applied load for Kumamoto andesite and HSULPC.

Fig. 5 K_I-da/dt relations for Kumamoto andesite in air at different temperature.

Fig. 6 K_I-da/dt relations for Kumamoto andesite in air at different relative humidity.

Fig. 7 K_I-da/dt relations for Kumamoto andesite in distilled water at different temperature.

Fig. 8 K_I-da/dt relations for HSULPC in air at different temperature.

Fig. 9 K_I-da/dt relations for HSULPC in air at different relative humidity.

Fig. 10 K_I-da/dt relations for HSULPC in water at different temperature.

Fig. 11 Relations between the long-term strength and time-to-failure for andesite and HSULPC.

(a): in air at the same relative humidity and different temperature

(b): in air at the same temperature and different relative humidity

(c): in water

Fig. 12 Relation between the temperature and n or log$A$ in air at constant relative humidity.

(a): relation between the temperature and n.

(b): relation between the temperature and log$A$.

Fig. 13 Relation between the relative humidity and n or log$A$ in air at constant temperature.

(a): relation between the relative humidity and n.

(b): relation between the relative humidity and log$A$.

Fig. 14 Relation between the temperature and n or log$A$ in water.

(a): relation between the temperature and n.

(b): relation between the temperature and log$A$.

Fig. 15 Relation between the long-term strength of HSULPC in 60000 years and environmental conditions.

(a): relation in air at constant relative humidity.

(b): relation in air at constant temperature.

(c): relation in water.

Tables

Table 1 The composition of HSULPC.

Contained amount [kg/m^3]	
low-heat portland cement	744 ~ 1014
silica fume	158 ~ 496
fillers (fly ash, blast furnace slag, etc.)	225 ~ 541
aggregates	631 ~ 947
water-reducing admixture	24
water	180

Table 2 Summary of the results for Kumamoto andesite in air at different temperature.

	logA	n	$K_I(10^{-6})$ [MN/m$^{3/2}$]	da/dt(1.4) [m/s]
293K, 55%	-15.8 (SD=1.8)	61 (SD=10)	1.45 (SD=0.01)	1.35×10^{-7} (SD=2.09×10^{0} in log)
329K, 50%	-13.3 (SD=0.5)	49 (SD=5)	1.41 (SD=0.03)	7.94×10^{-7} (SD=2.88×10^{0} in log)
348K, 50%	-11.8 (SD=0.2)	43 (SD=1)	1.36 (SD=0.00)	3.63×10^{-6} (SD=1.02×10^{0} in log)

SD: standard deviation

Table 3 Summary of the results for Kumamoto andesite in air at different relative humidity.

	logA	n	$K_I(10^{-6})$ [$MN/m^{3/2}$]	da/dt(1.5) [m/s]
292K, 25%	-17.2 (SD=2.2)	58 (SD=9)	1.56 (SD=0.03)	1.07×10^{-7} (SD=4.79×10^{0} in log)
293K, 89%	-1.0 (SD=2.3)	45 (SD=4)	1.37 (SD=0.04)	6.03×10^{-5} (SD=2.82×10^{0} in log)

SD: standard deviation

Table 4 Summary of the results for Kumamoto andesite in distilled water.

	logA	n	$K_I(10^{-6})$ [$MN/m^{3/2}$]	da/dt(1.1) [m/s]
285K pH=6~7	-7.6 (SD=0.5)	41 (SD=2)	1.10 (SD=0.03)	1.15×10^{-6} (SD=3.16×10^{0} in log)
328K pH=5	-6.1 (SD=0.6)	32 (SD=2)	1.01 (SD=0.04)	1.91×10^{-5} (SD=3.89×10^{0} in log)

SD: standard deviation

Table 5 Summary of the results for HSULPC in air at different temperature.

	logA	n	$K_I(10^{-6})$ [$MN/m^{3/2}$]	da/dt(1.3) [m/s]
284K, 52%	-23.7 (SD=3.1)	149 (SD=35)	1.31 (SD=0.03)	1.75×10^{-7} ($SD=1.23\times10^{1}$ in log)
329K, 52%	-18.6 (SD=2.3)	101 (SD=9)	1.32 (SD=0.06)	1.44×10^{-7} ($SD=8.51\times10^{1}$ in log)
348K, 50%	-19.3 (SD=3.0)	100 (SD=12)	1.36 (SD=0.08)	1.24×10^{-8} ($SD=7.59\times10^{2}$ in log)

SD: standard deviation

Table 6 Summary of the results for HSULPC in water at different relative humidity.

	logA	n	$K_I(10^{-6})$ [$MN/m^{3/2}$]	da/dt(1.35) [m/s]
291K, 26%	-36.6 (SD=8.2)	228 (SD=35)	1.36 (SD=0.05)	1.10×10^{-7} ($SD=6.92\times10^{3}$ in log)
293K, 89%	-26.0 (SD=3.4)	152 (SD=18)	1.35 (SD=0.04)	6.31×10^{-7} ($SD=5.75\times10^{1}$ in log)

SD: standard deviation

Table 7 Summary of the results for HSULPC in water.

	logA	n	$K_I(10^{-6})$ [$MN/m^{3/2}$]	da/dt(1.1) [m/s]
285K pH=10	-18.7 (SD=4.0)	138 (SD=41)	1.24 (SD=0.02)	9.77×10^{-14} ($SD=2.63\times10^{2}$ in log)
326K pH=9~10	-8.6 (SD=1.0)	88 (SD=18)	1.07 (SD=0.04)	1.23×10^{-5} ($SD=3.98\times10^{1}$ in log)
346K pH=9	-5.7 (SD=0.2)	53 (SD=9)	0.99 (SD=0.01)	3.55×10^{-4} ($SD=3.89\times10^{0}$ in log)

SD: standard deviation

Fig. 1

Click here to download high resolution image

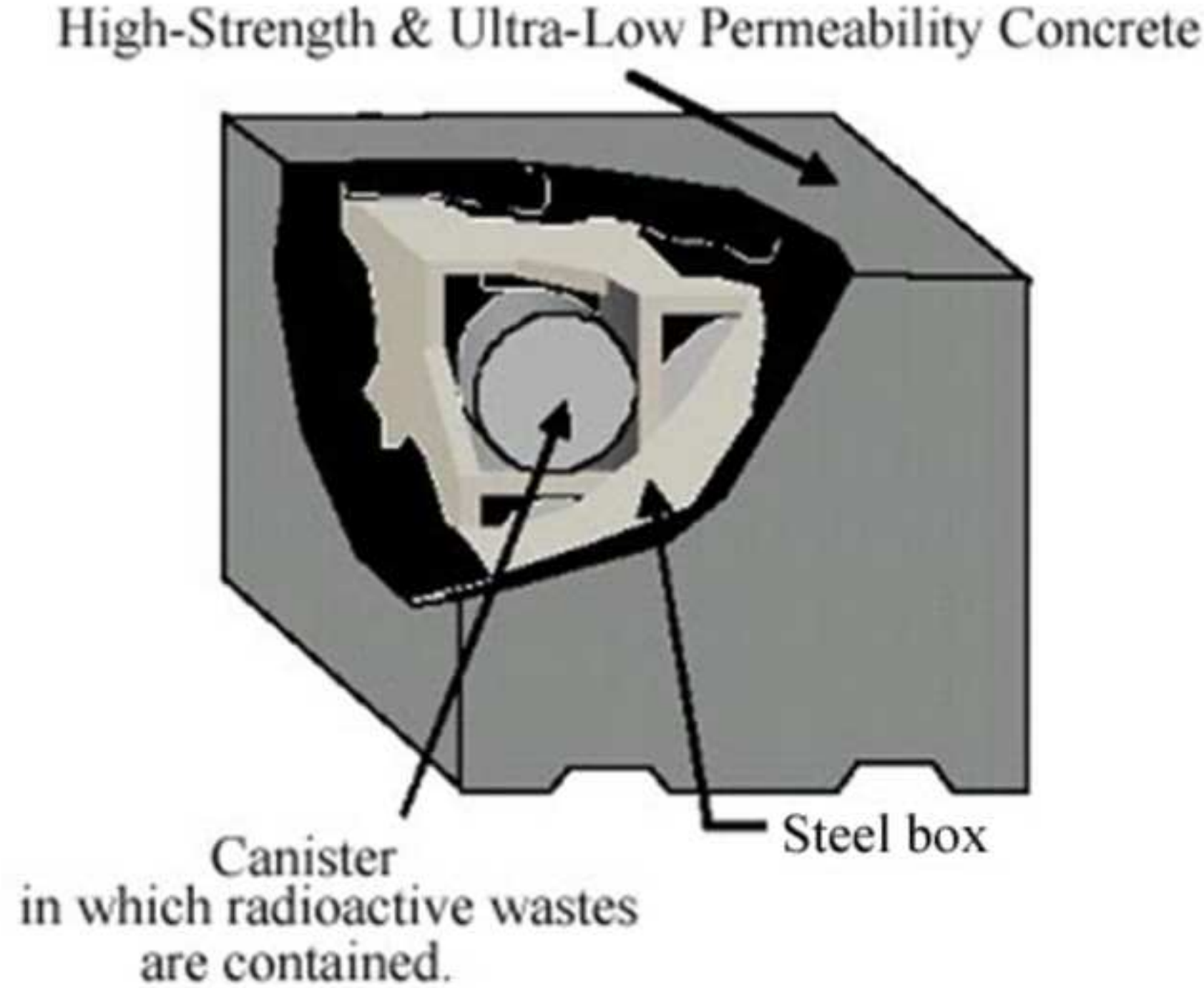

Fig. 2

Click here to download high resolution image

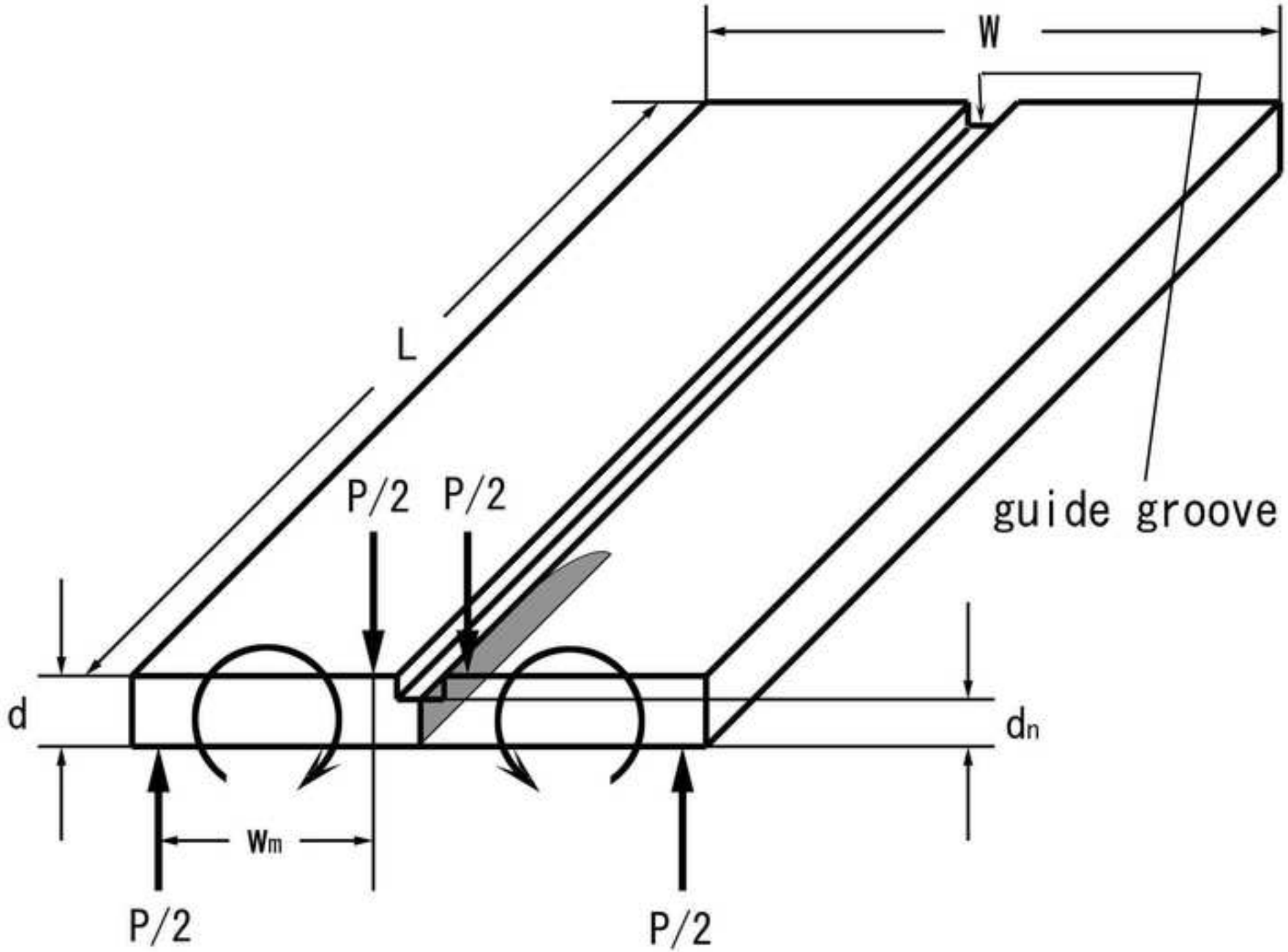

Fig. 3

Click here to download high resolution image

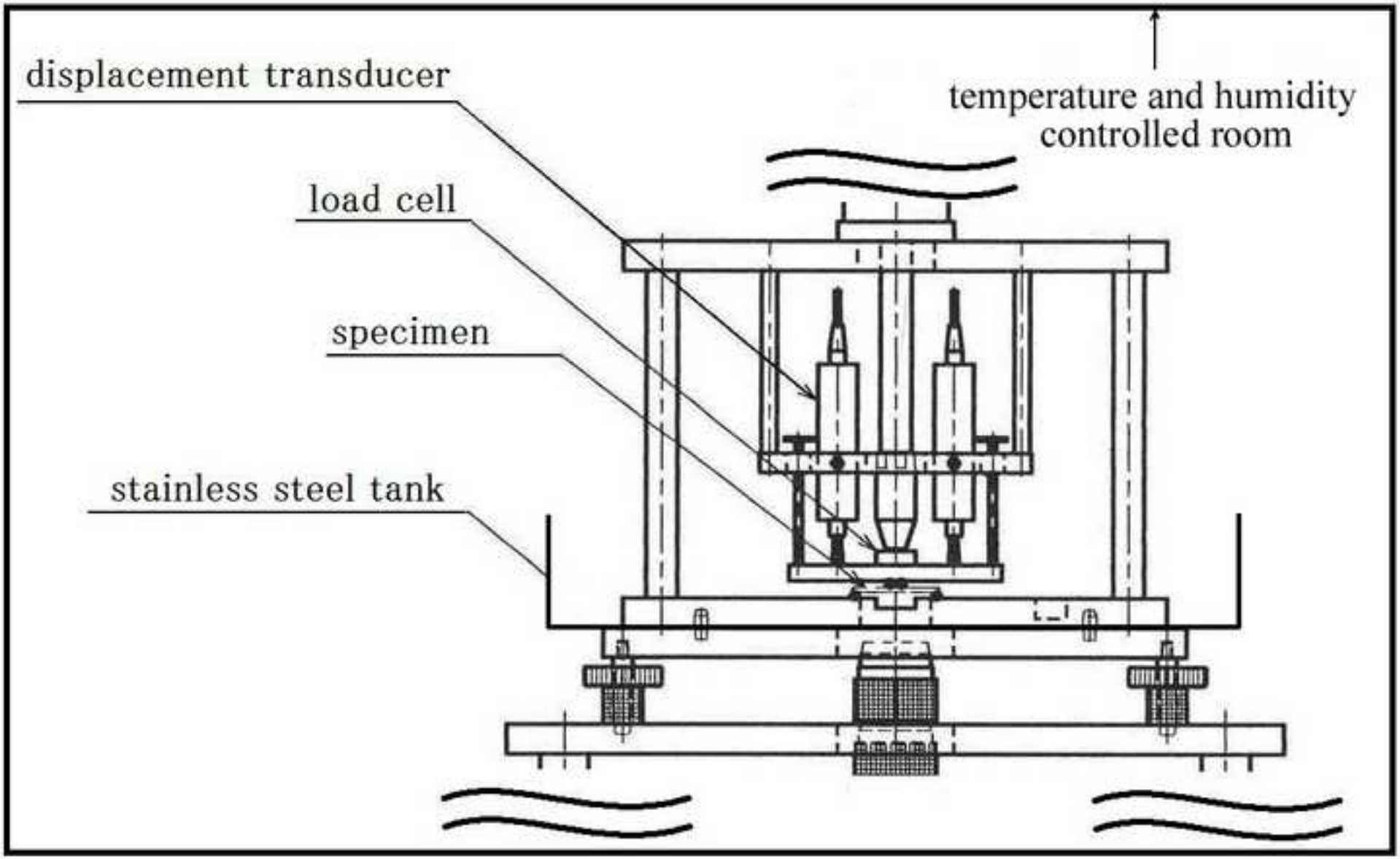

Fig. 4

Click here to download high resolution image

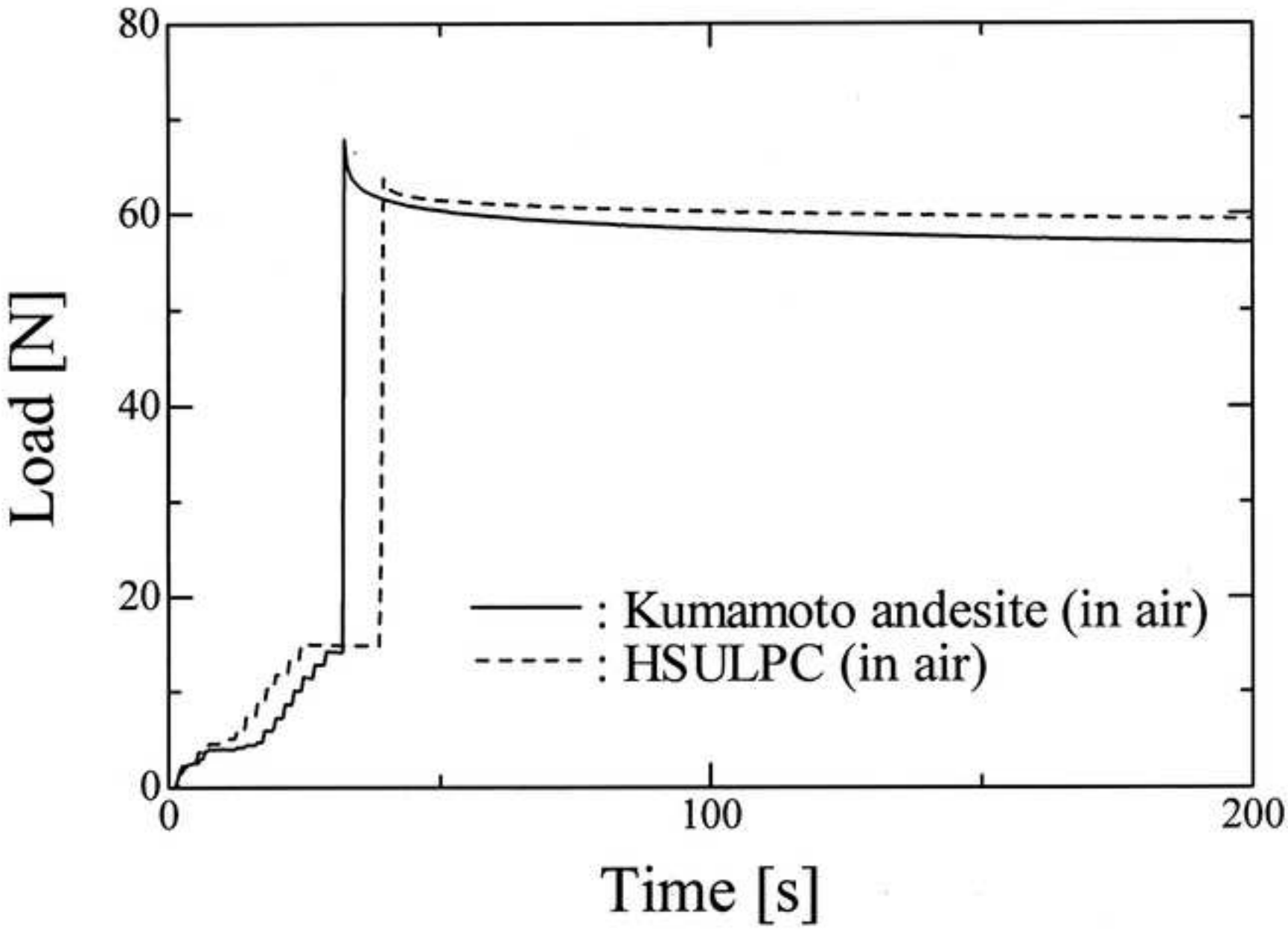

Fig. 5

Click here to download high resolution image

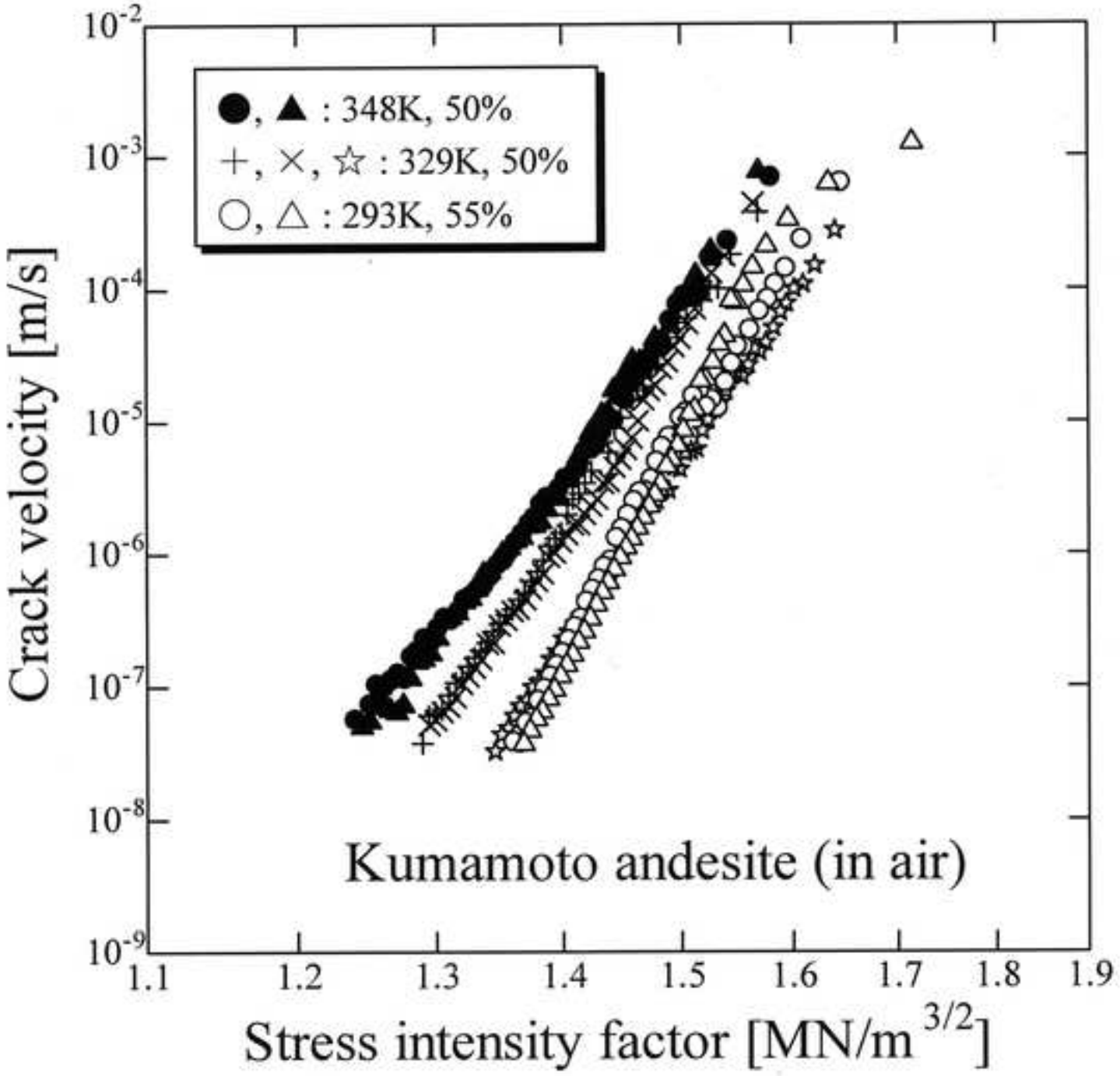

Fig. 6

Click here to download high resolution image

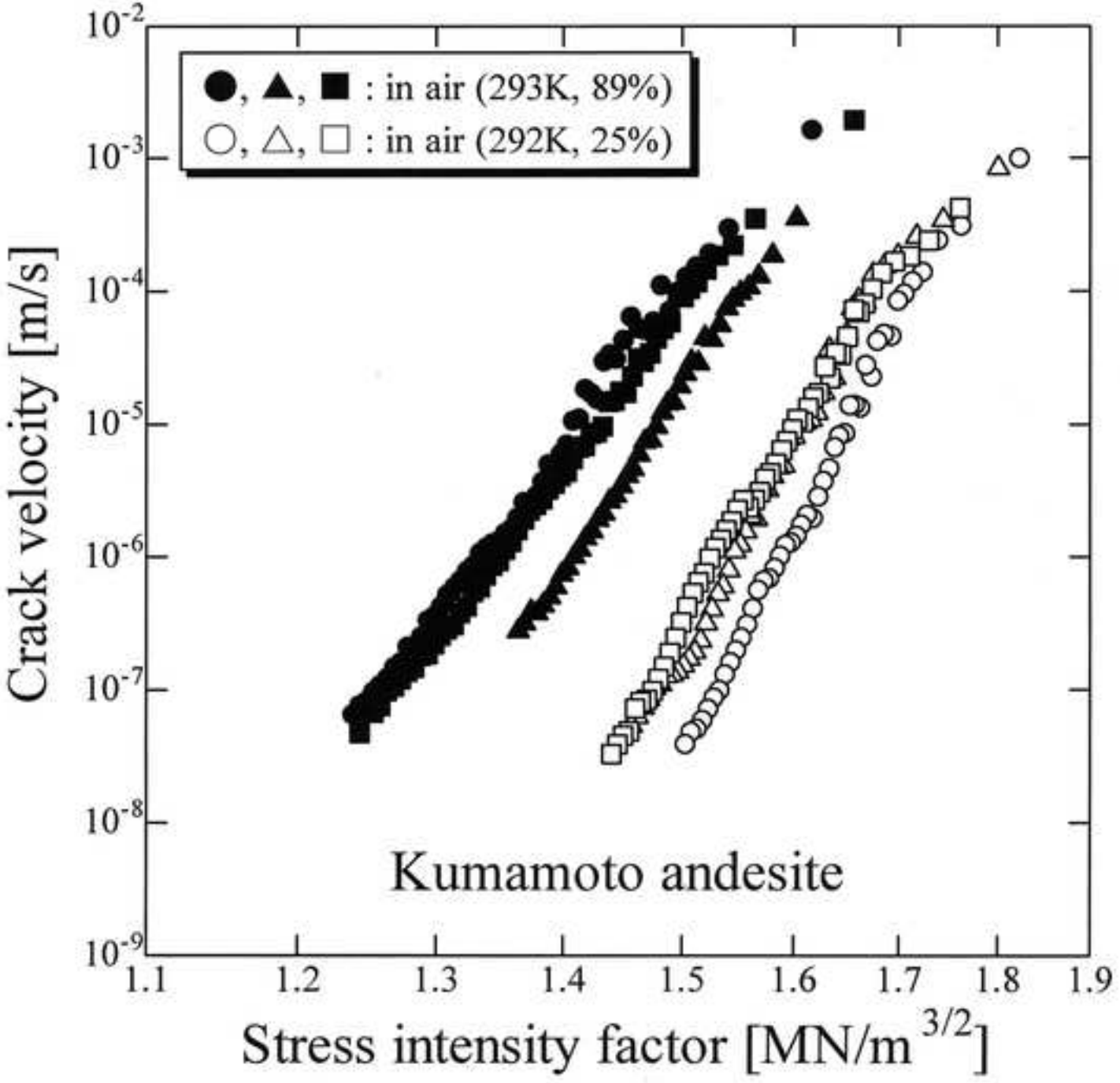

Fig. 7

Click here to download high resolution image

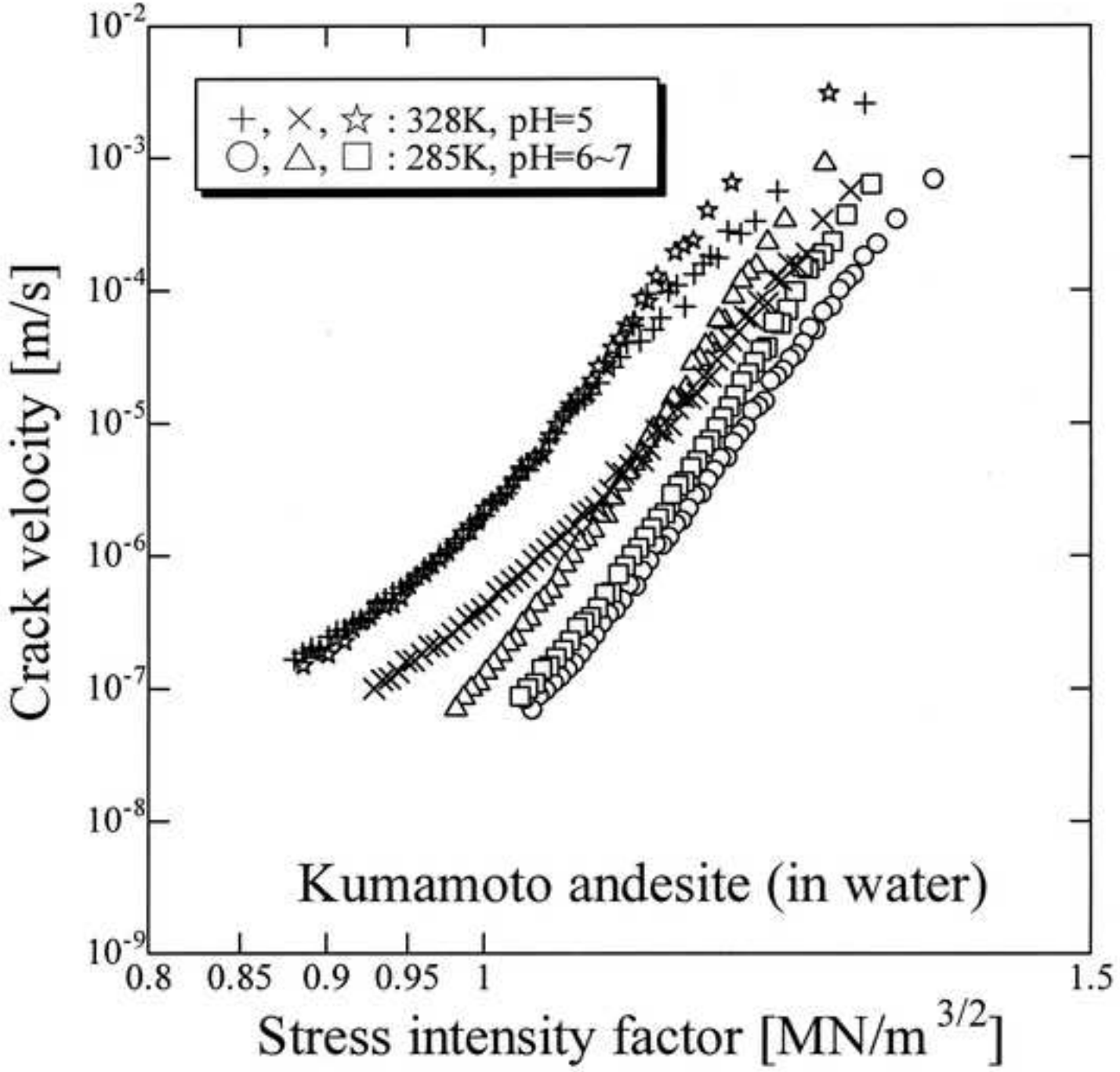

Fig. 8

Click here to download high resolution image

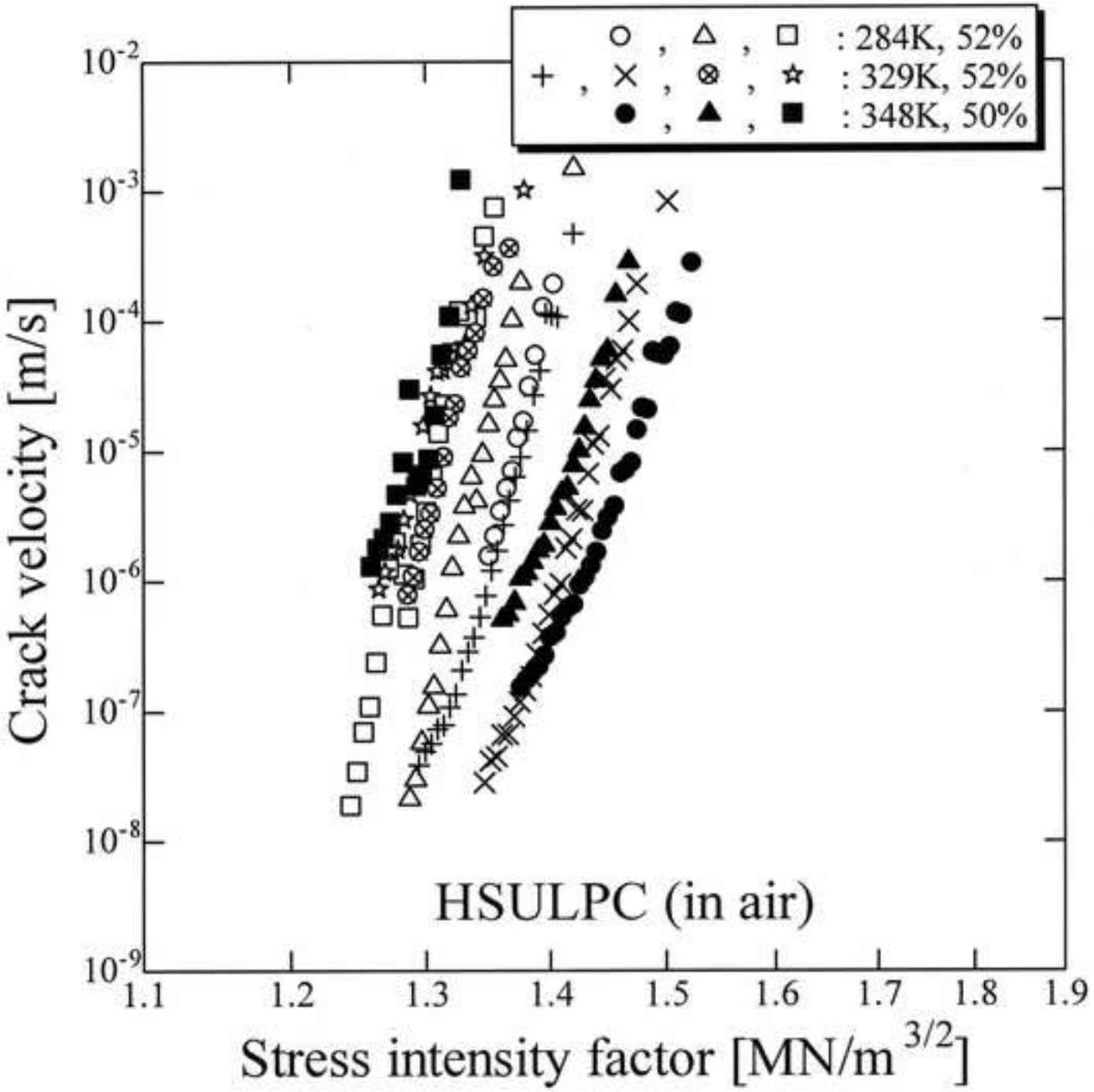

Fig. 9

Click here to download high resolution image

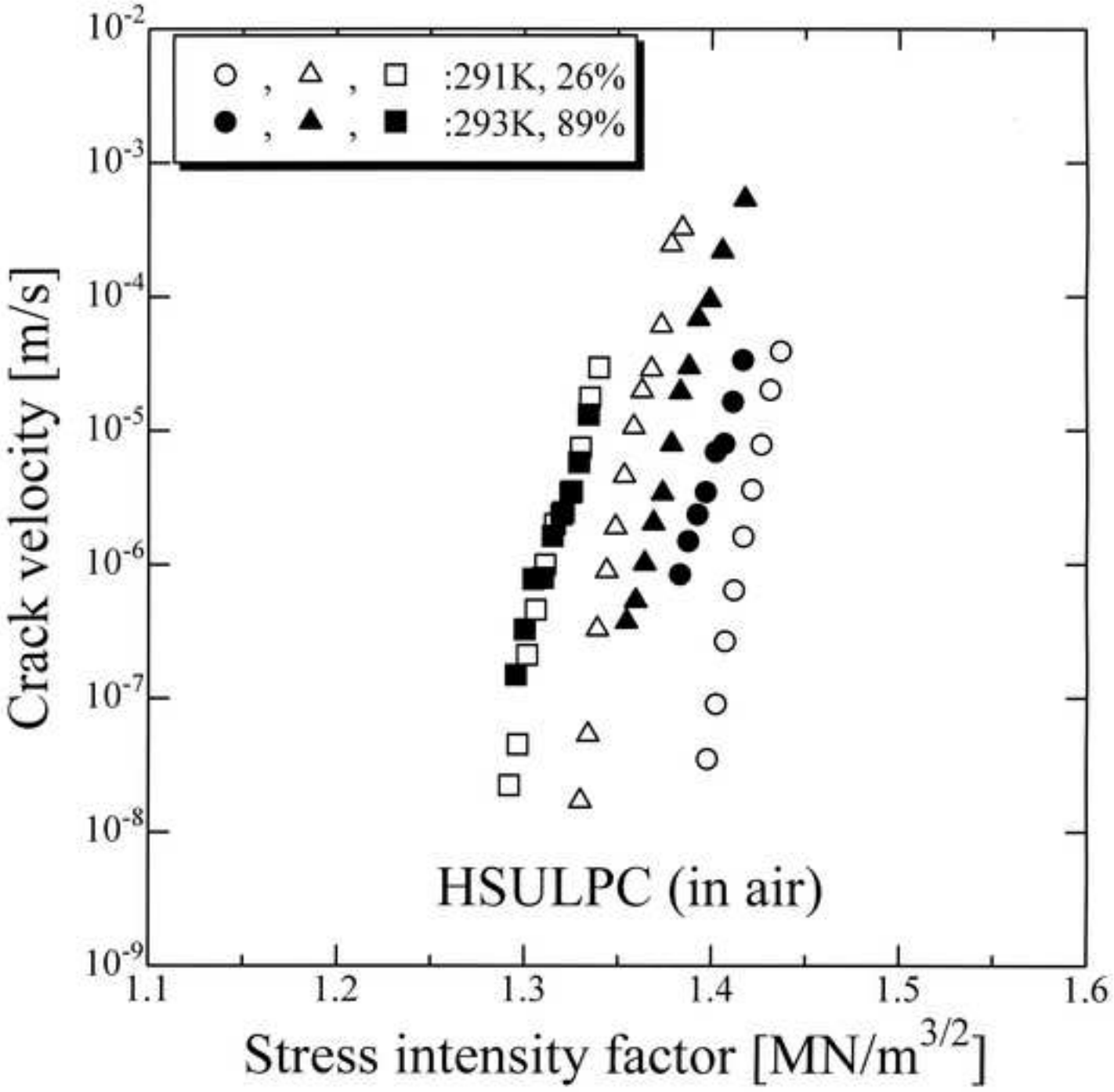

Fig. 10

Click here to download high resolution image

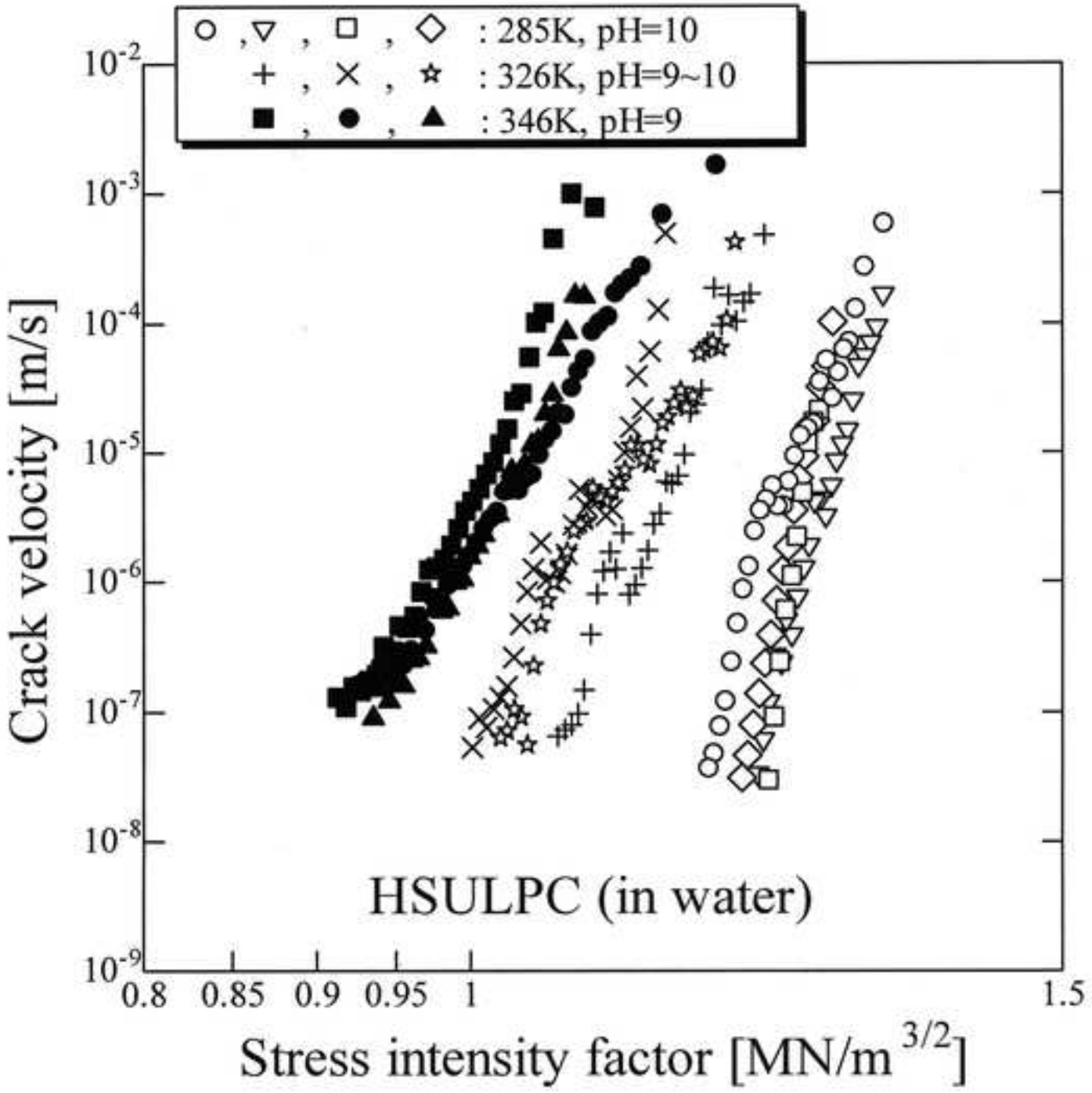

Fig. 11(a)
Click here to download high resolution image

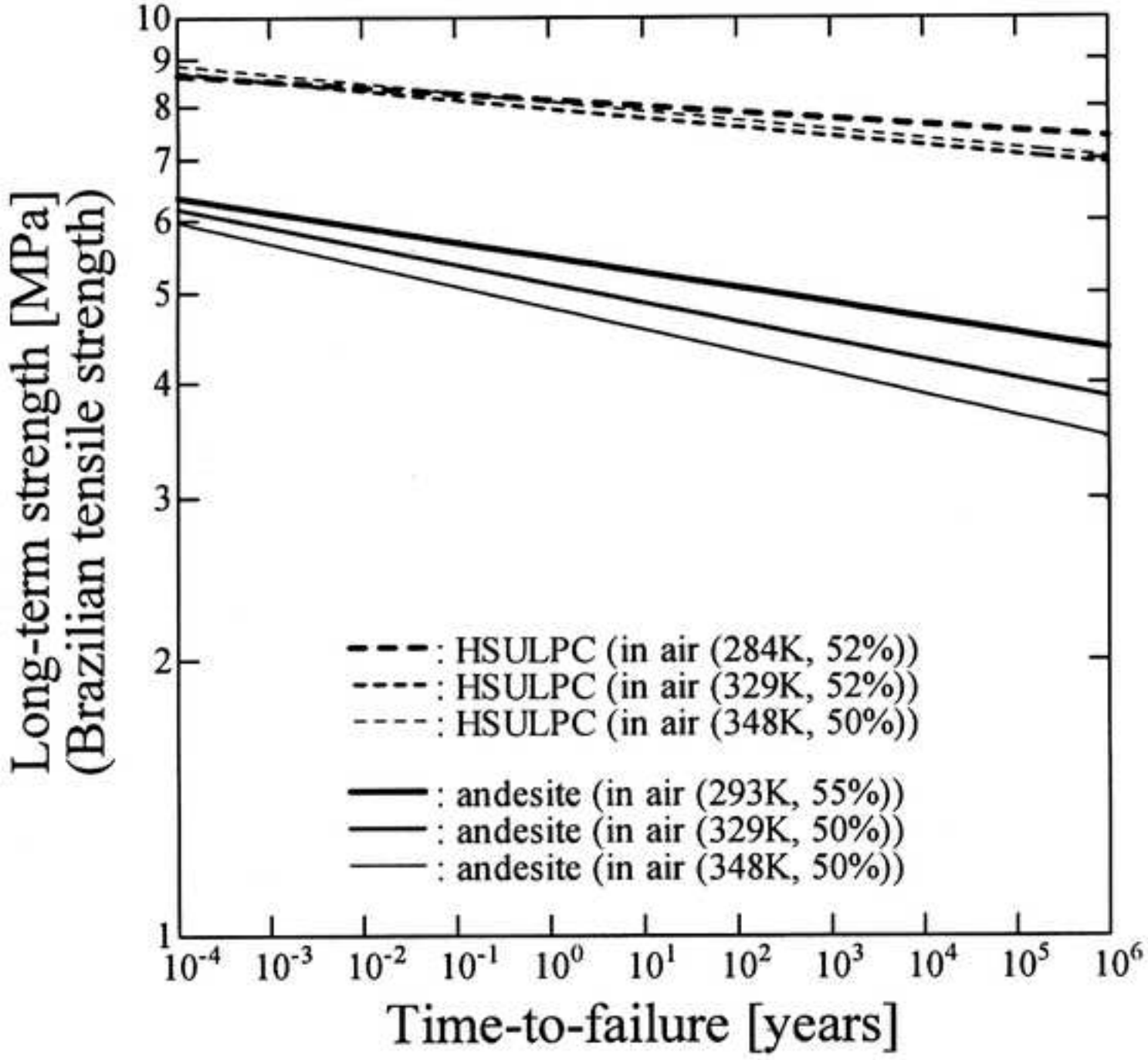

Fig. 11(b)

Click here to download high resolution image

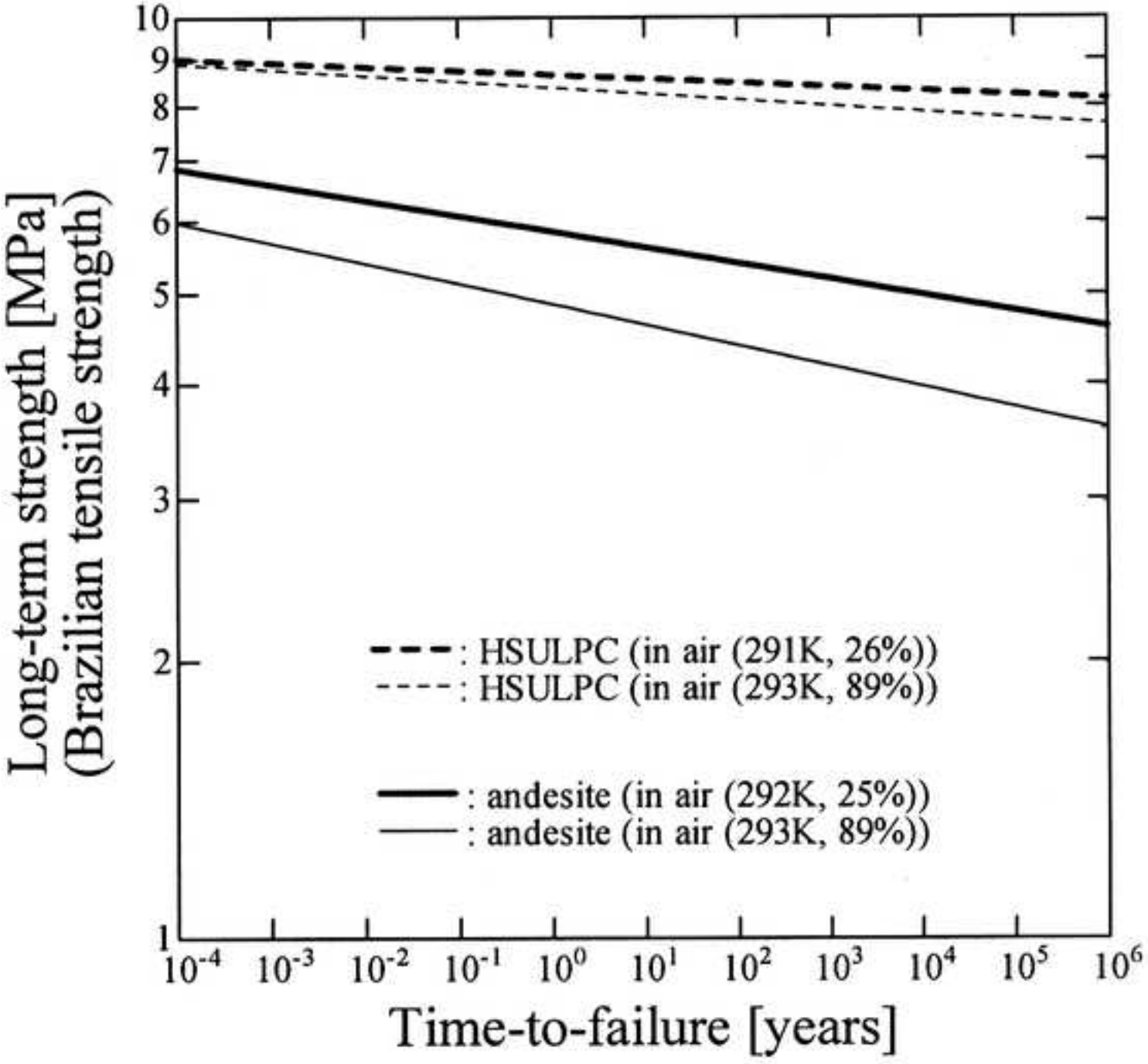

Fig. 11(c)
Click here to download high resolution image

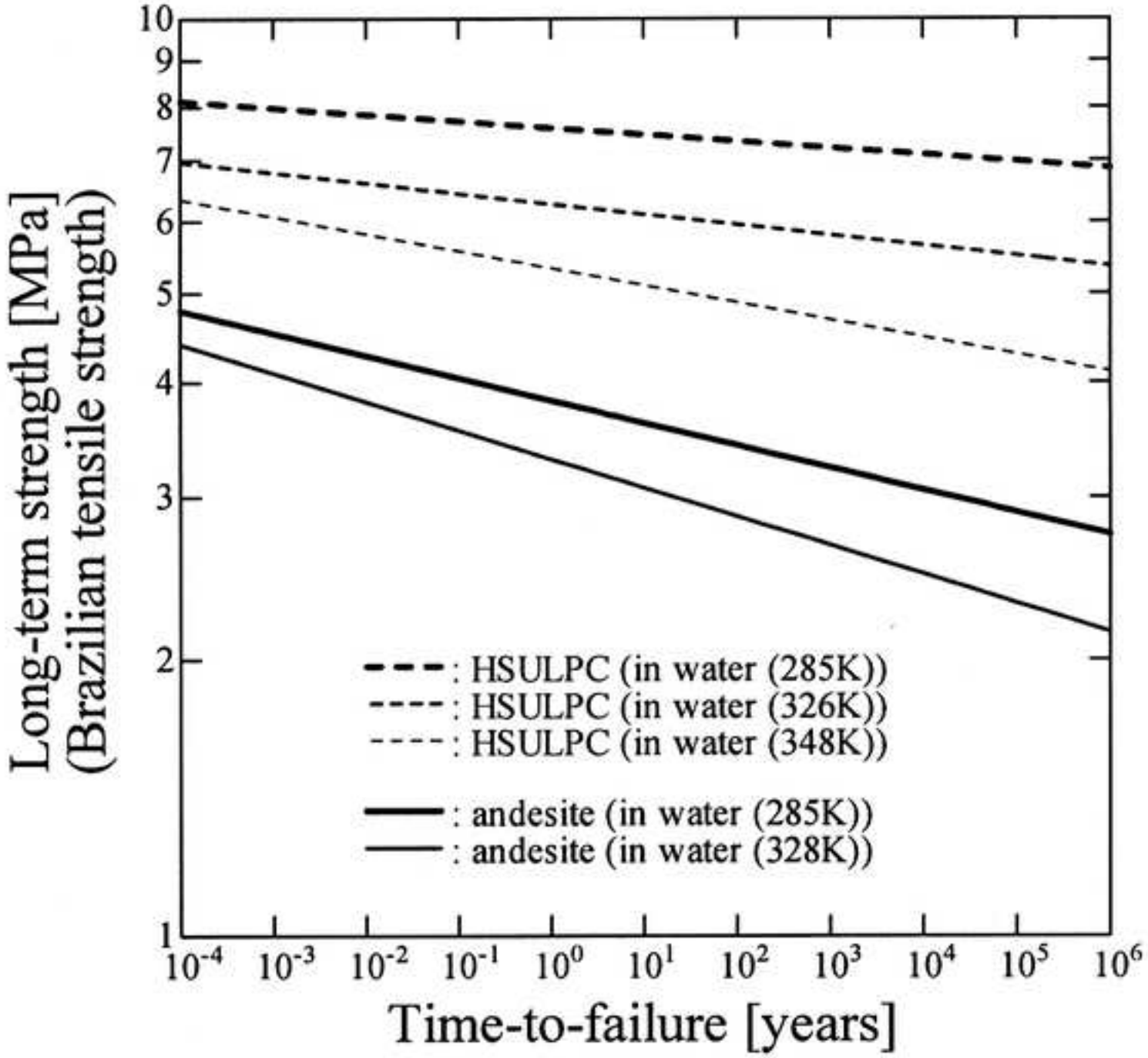

Fig. 12(a)
Click here to download high resolution image

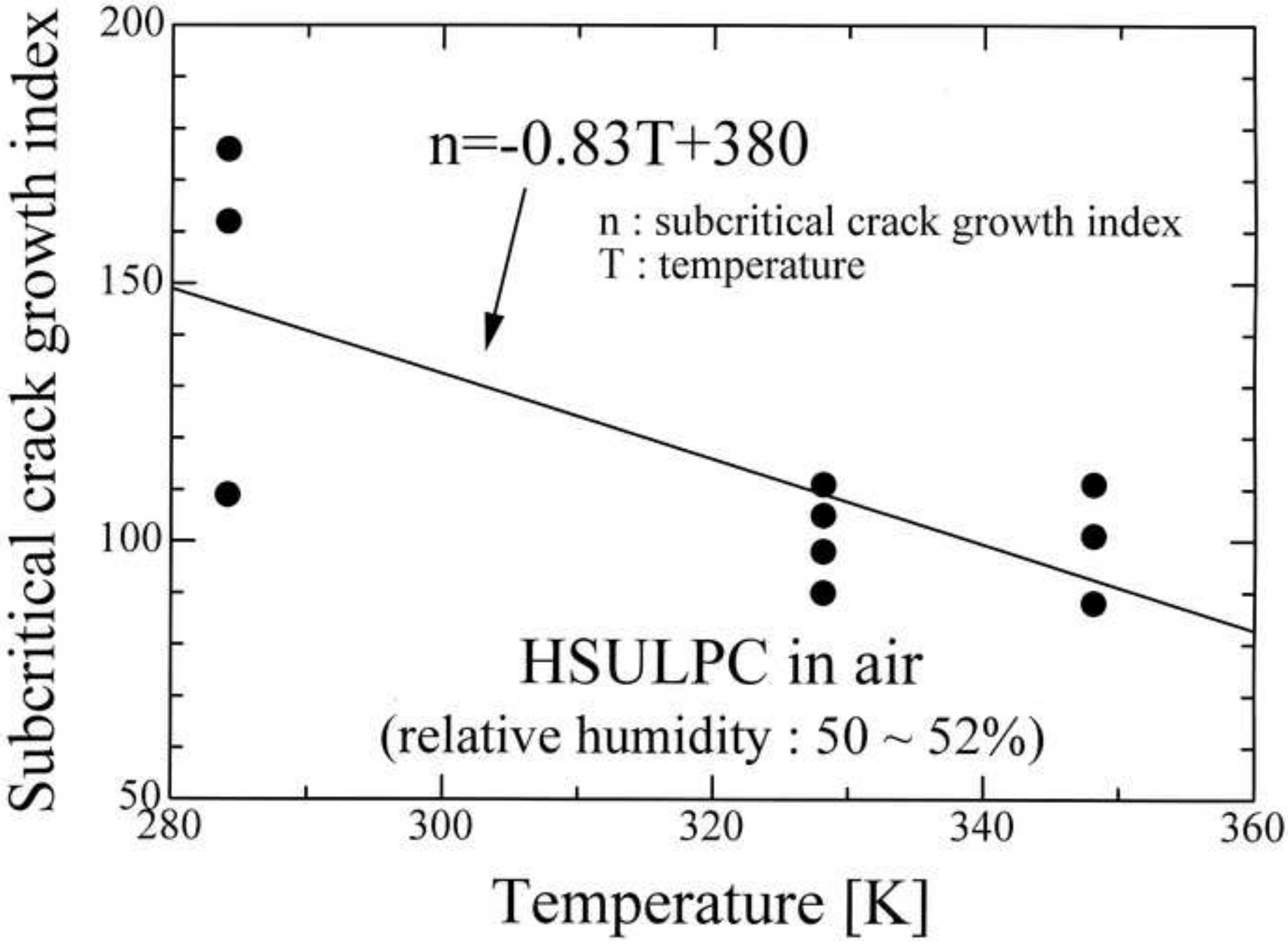

Fig. 12(b)
Click here to download high resolution image

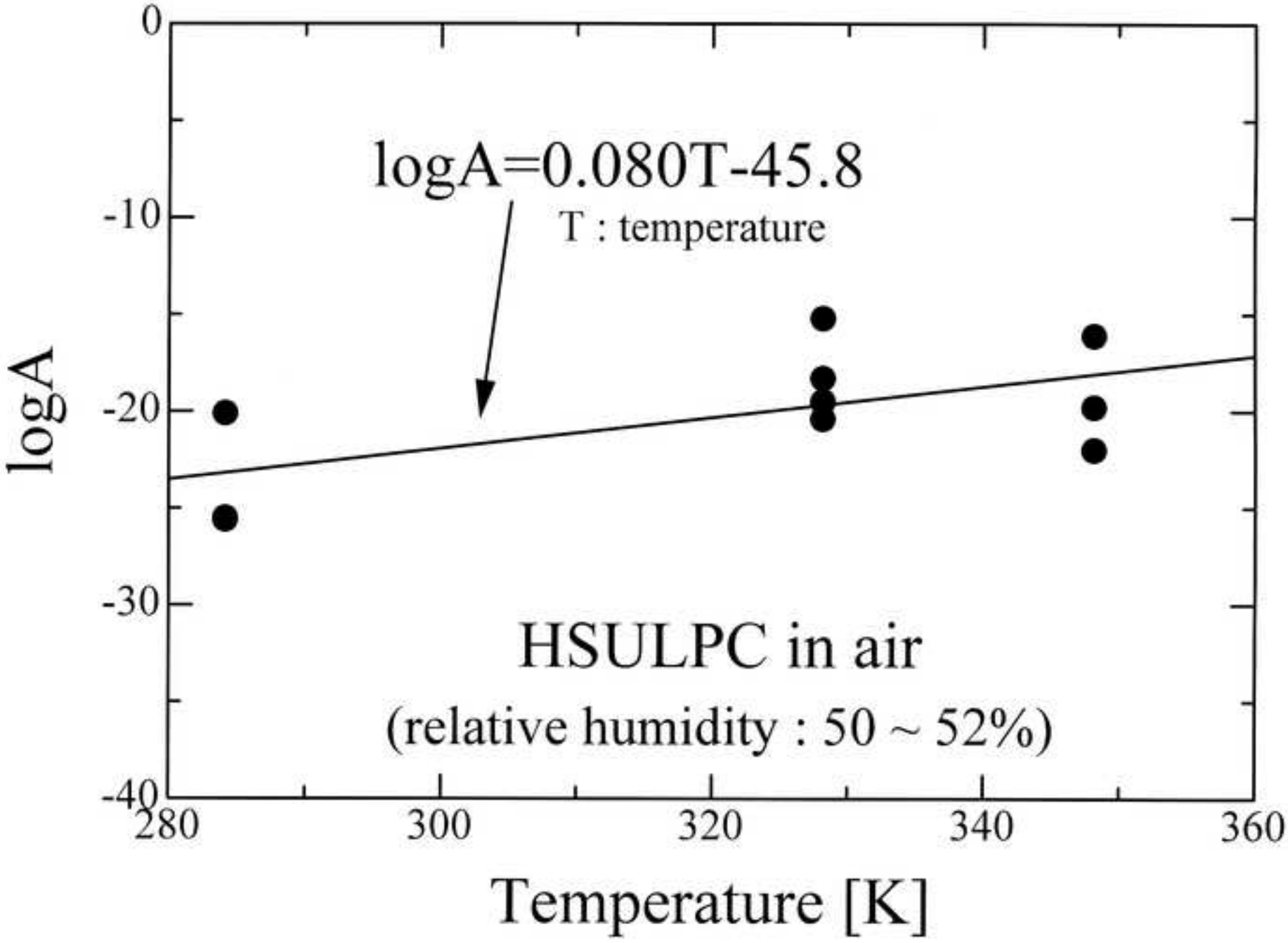

Fig. 13(a)
Click here to download high resolution image

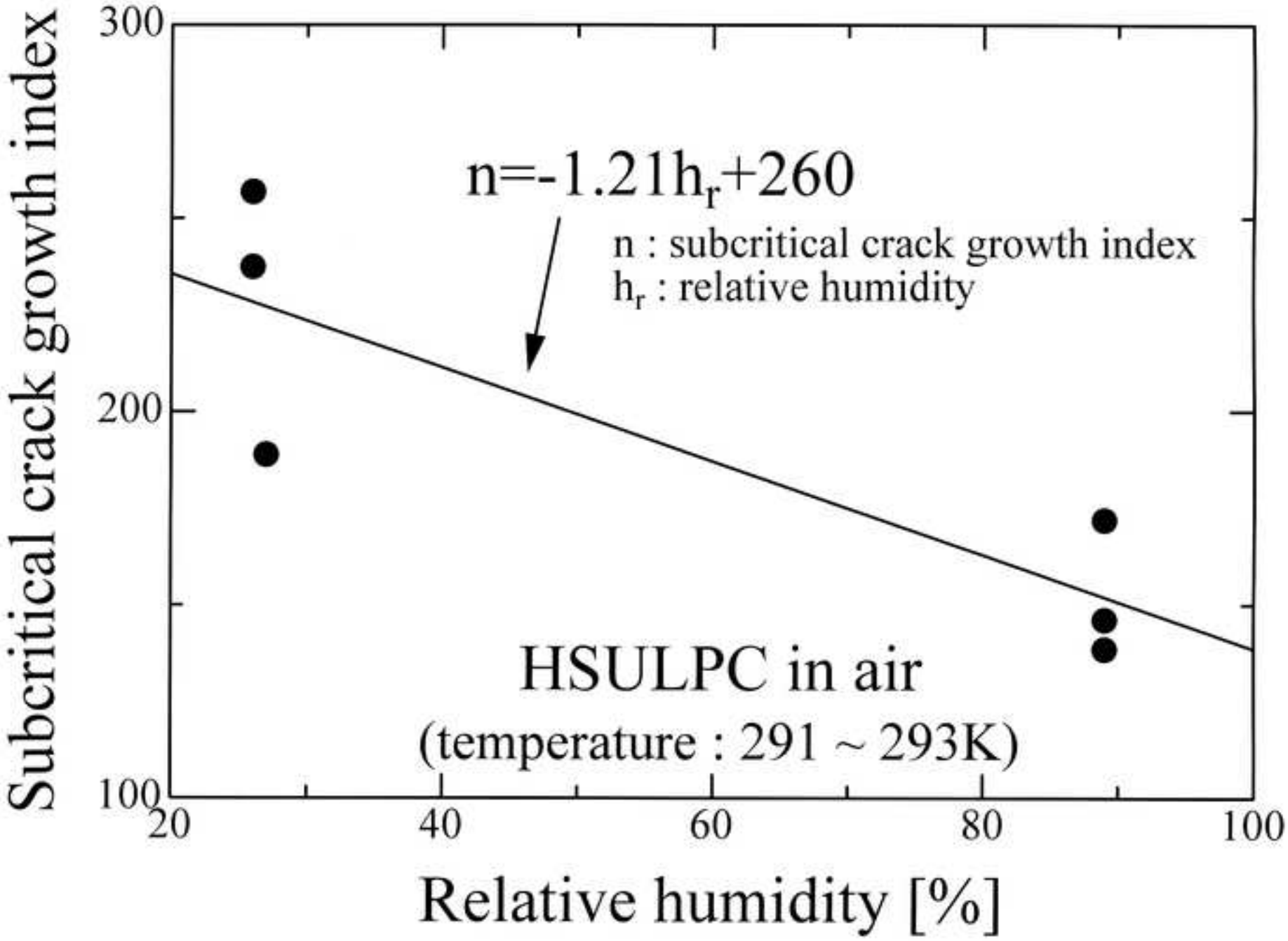

Fig. 13(b)
Click here to download high resolution image

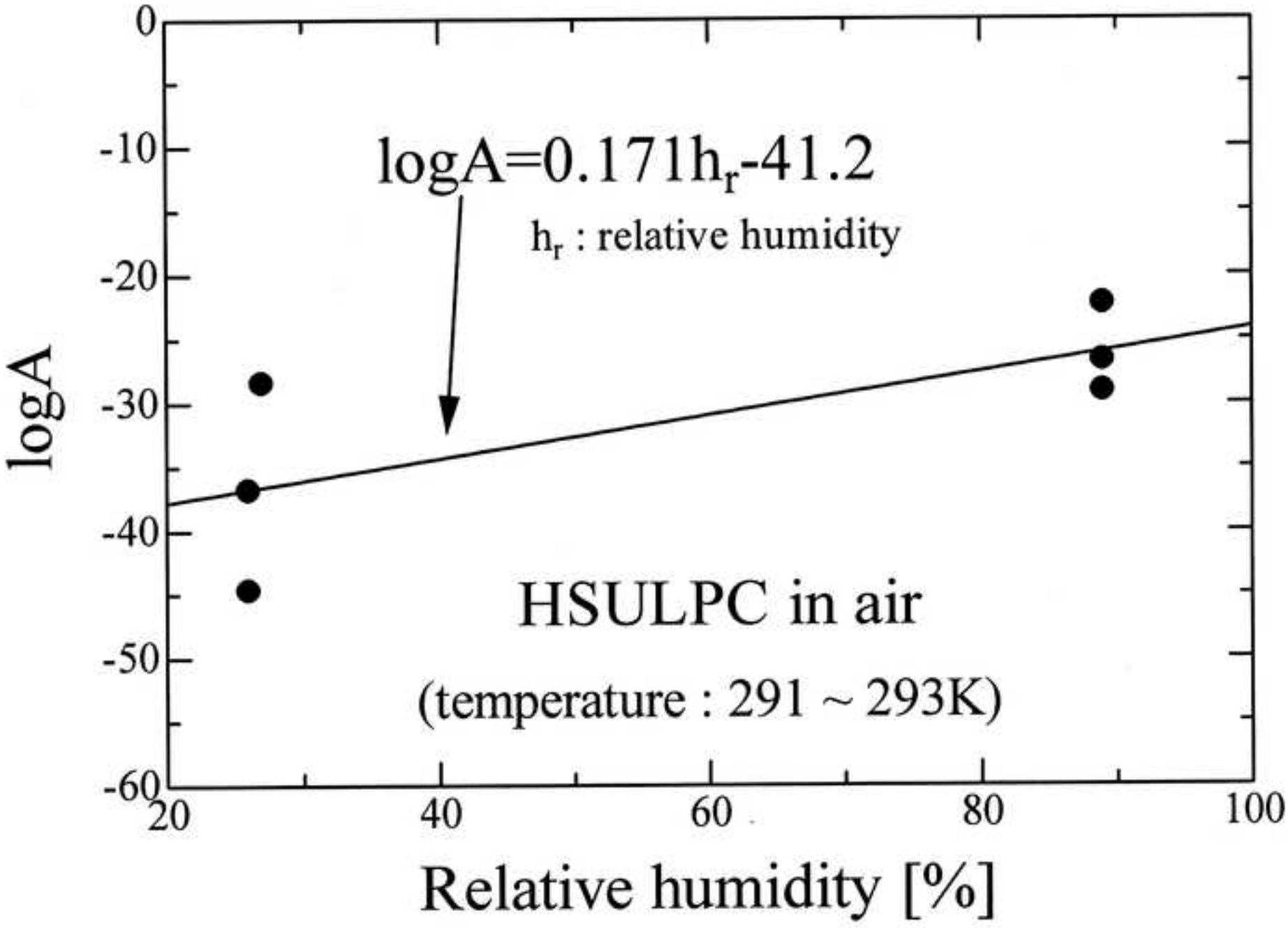

Fig. 14(a)

Click here to download high resolution image

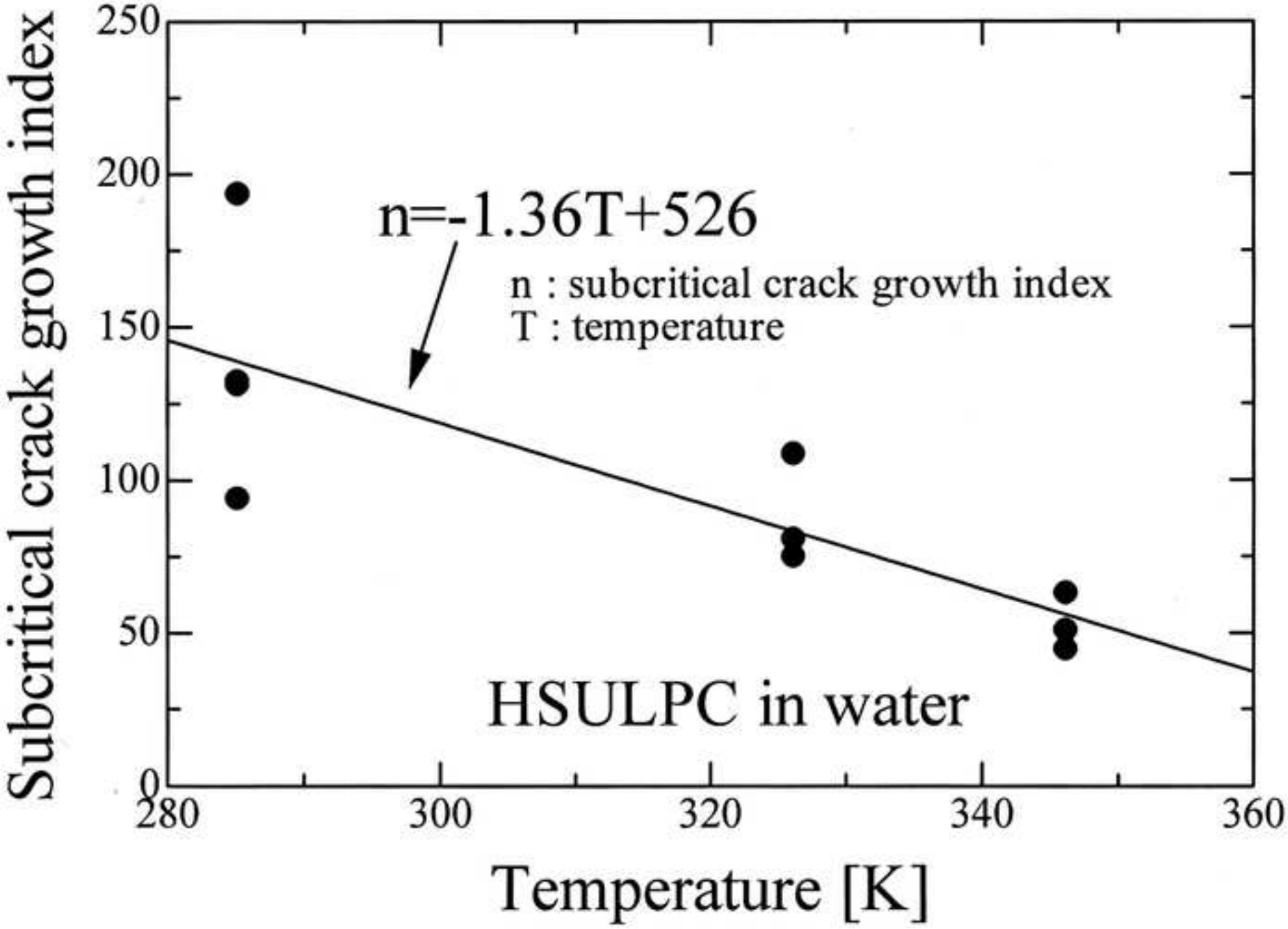

Fig. 14(b)
Click here to download high resolution image

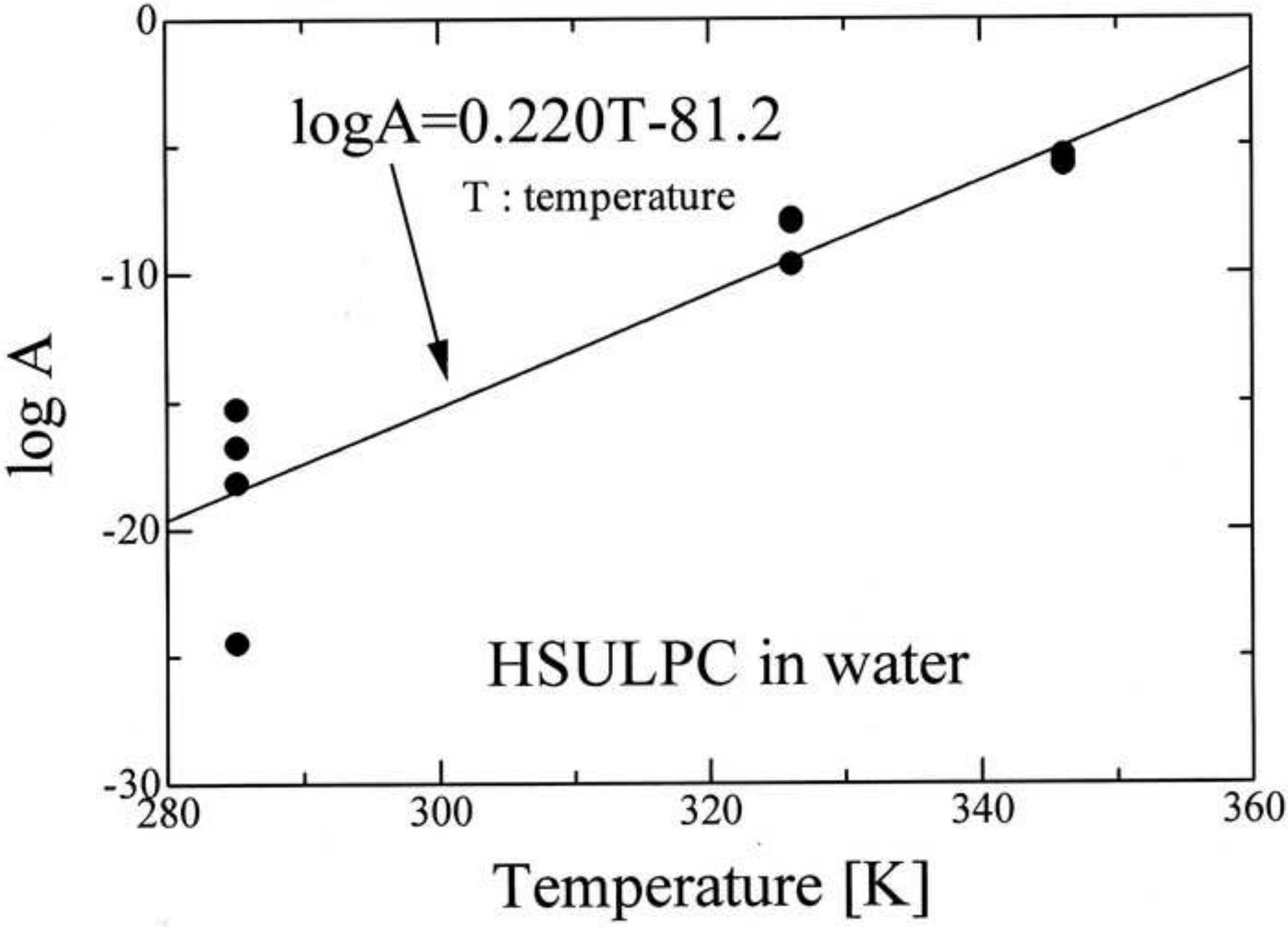

Fig. 15(a)
Click here to download high resolution image

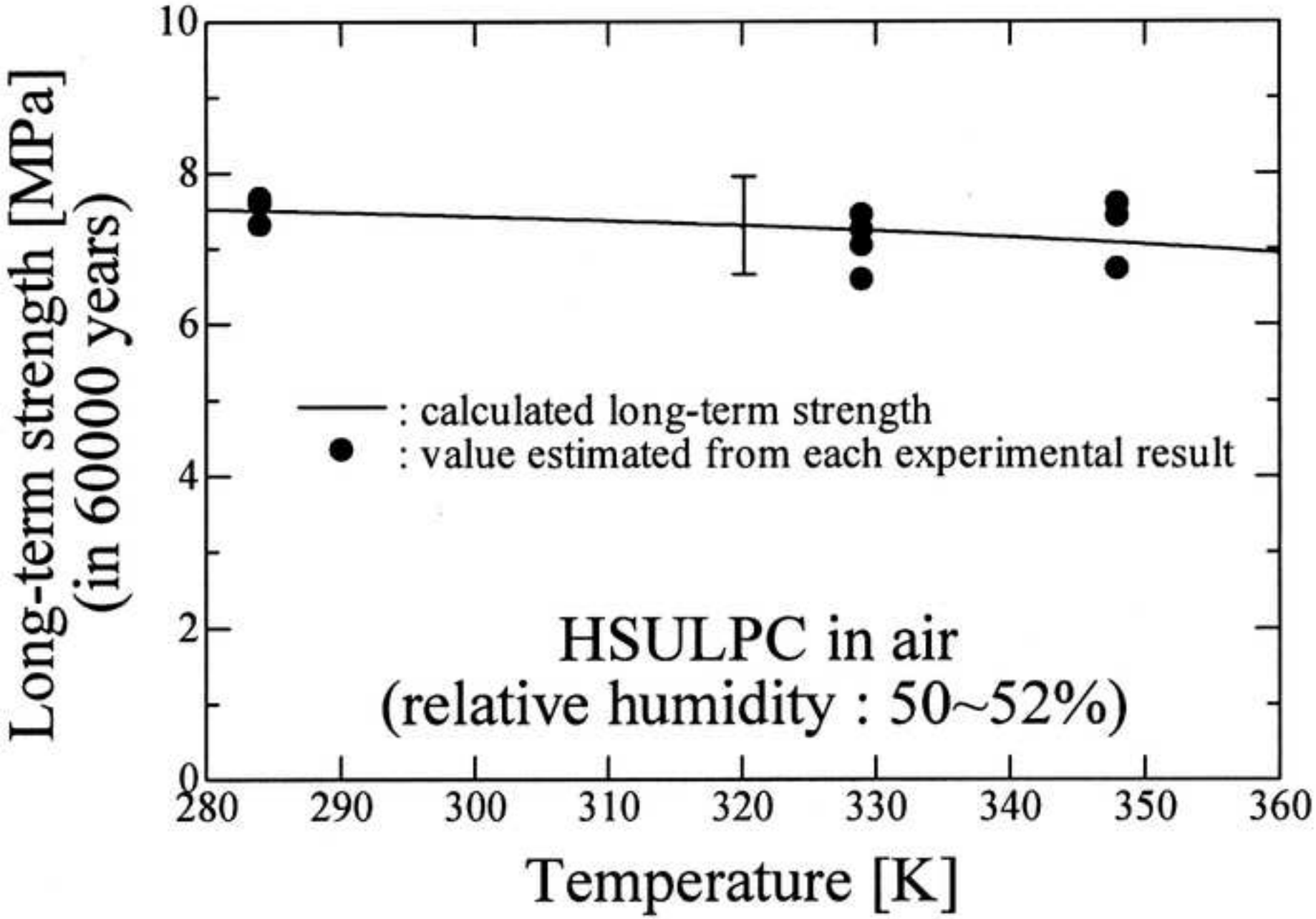

Fig. 15(b)
Click here to download high resolution image

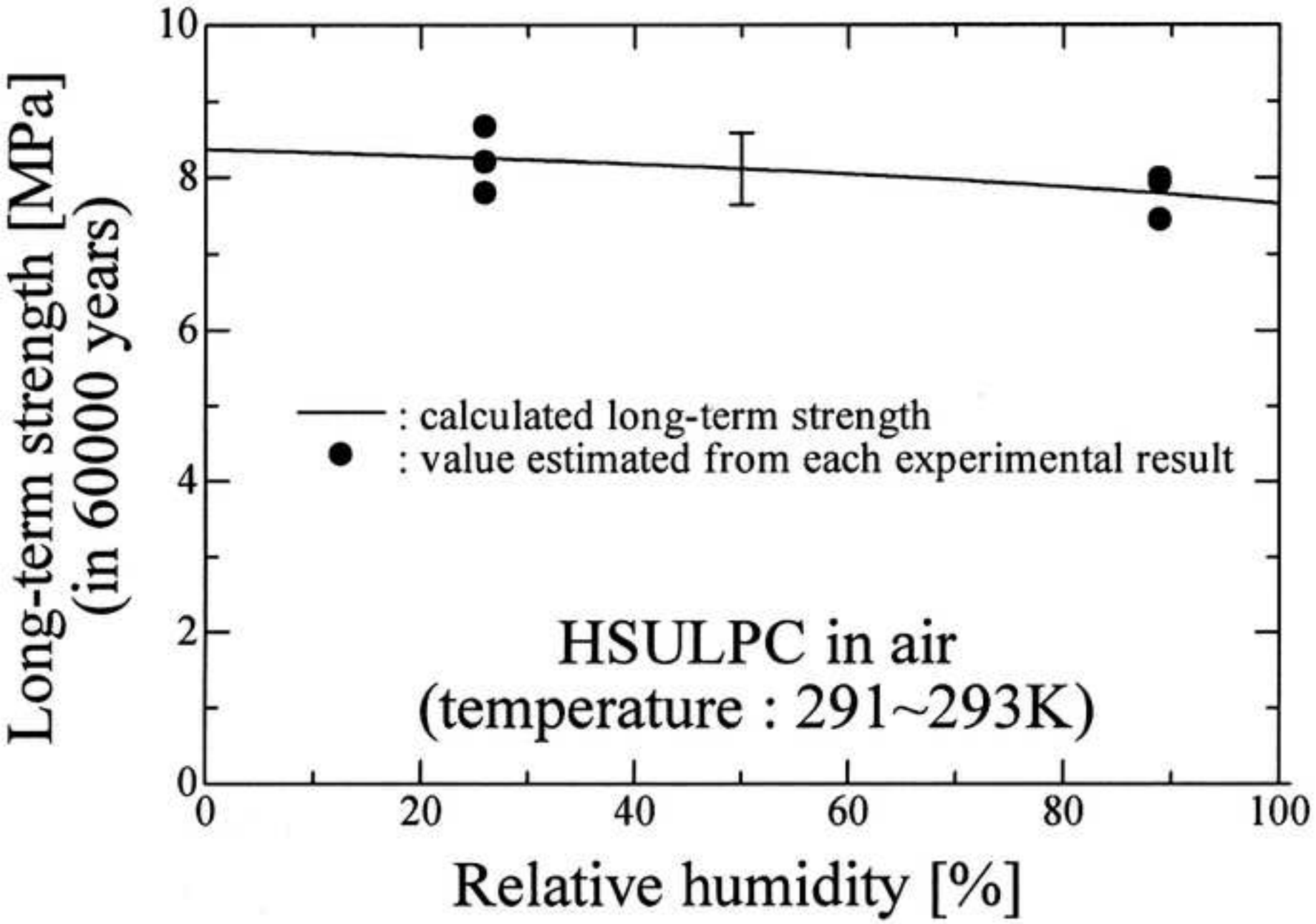

Fig. 15(c)
Click here to download high resolution image